

LA-5582-PR

Progress Report

*c. 1*

Quarterly Report

# Advanced Plutonium Fuels Program

October 1 through December 31, 1973

L



## For Reference

Not to be taken from this room



This report was prepared as an account of work sponsored by the United States Government. Neither the United States nor the United States Atomic Energy Commission, nor any of their employees, nor any of their contractors, subcontractors, or their employees, makes any warranty, express or implied, or assumes any legal liability or responsibility for the accuracy, completeness or usefulness of any information, apparatus, product or process disclosed, or represents that its use would not infringe privately owned rights.

This report presents the status of the Advanced Plutonium Fuels Program. The four most recent reports in this series, unclassified, are:

LA-5193-PR  
LA-5284-PR

LA-5390-PR  
LA-5477-PR

In the interest of prompt distribution, this progress report was not edited by the Technical Information staff.

Printed in the United States of America. Available from  
National Technical Information Service  
U.S. Department of Commerce  
5285 Port Royal Road  
Springfield, Virginia 22151  
Price: Printed Copy \$4.00 Microfiche \$1.45

LA-5582-PR  
Progress Report  
UC-79b  
Issued: April 1974



Quarterly Report  
**Advanced Plutonium Fuels Program**  
October 1 through December 31, 1973

Compiled by

**R. D. Baker**



This work supported by the U.S. Atomic Energy Commission's Division of Reactor Research and Development.

TABLE OF CONTENTS

<u>PROJECT</u>		<u>PAGE</u>
401	EXAMINATION OF FAST REACTOR FUELS	
	I. Introduction	1
	II. Equipment Development	1
	III. Analytical Chemistry	3
	IV. Microstructural Analysis	4
	V. Requests from DRRD	4
	VI. Quality Assurance	6
	VII. References	7
	VIII. Publications	7
463	HIGH PERFORMANCE LMFBR FUEL MATERIALS	
	I. Introduction	8
	II. Irradiation Testing	8
	III. Quality Assurance	23
	IV. References	23
472	FBR ANALYTICAL QUALITY ASSURANCE STANDARDS AND METHODS RESEARCH AND DEVELOPMENT	
	I. Introduction	25
	II. Analytical Chemistry Program For Low-Friction, Hard Surfaces	25
	III. Analytical Chemistry Program For Metallic Core Components	27
	IV. Analytical Chemistry Program For Boron Carbide	28
	V. Analytical Chemistry Program For FBR Mixed Oxide Fuel	28
	VI. Quality Assurance	29
	VII. References	30
	VIII. Publications, Talks	30

## ABSTRACT

This is the 29th quarterly report on the Advanced Plutonium Fuels Program at the Los Alamos Scientific Laboratory.

Most of the investigations discussed here are of the continuing type. Results and conclusions described may therefore be changed or augmented as the work continues. Published reference to results cited in this report should not be made without obtaining explicit permission to do so from the person in charge of the work.

## PROJECT 401

### EXAMINATION OF FAST REACTOR FUELS

Person in Charge: R. D. Baker  
Principal Investigators: J. W. Schulte  
K. A. Johnson  
G. R. Waterbury

---

#### I. INTRODUCTION

This project is directed toward the examination and comparison of the effects of neutron irradiation on LMFBR Program fuel materials. Unirradiated and irradiated materials will be examined as requested by the Fuels and Materials Branch of DRRD. Capabilities are established and are being expanded for providing conventional preirradiation and postirradiation examinations. Nondestructive tests will be conducted in a hot cell facility specifically modified for examining irradiated prototype fuel pins at a rate commensurate with schedules established by DRRD.

Characterization of unirradiated and irradiated fuels by analytical chemistry methods will continue, and additional methods will be modified and mechanized for hot cell application. Macro- and micro-examinations will be made on fuel and cladding using the shielded electron microprobe, emission spectrograph, radiochemistry, gamma scanner, mass spectrometers, and other analytical facilities. New capabilities will be developed in gamma scanning, analyses to assess spatial distributions of fuel and fission products, mass spectrometric measurements of burnup and fission gas constituents, chemical analyses, and measurement of carbon in irradiated fuels.

Microstructural analyses of unirradiated and irradiated materials will continue using optical and electron microscopy, and autoradiographic and x-ray techniques. Special emphasis will be placed on numerical

representation of microstructures and its relationship to fabrication and irradiation parameters. New etching and mounting techniques will be developed for high burnup materials.

#### II. EQUIPMENT DEVELOPMENT

##### A. In-Cell Equipment

(R. W. Basinger, G. R. Brewer, F. J. Fitzgibbon, M. E. Lazarus, P. A. Mason, F. H. Newbury, W. T. Wood)

##### 1. System for Obtaining Weight and Density of Fuel Pins

The fill and drain system to permit using a suitable fluid in the submersion of fuel pins for density determination has been installed.

##### 2. Slurper Drain Filter Assembly

A new design filter assembly has been designed and installed in the Slurper Drains of the Metallography Cells. The filter utilizes a disposable package concept for easier replacement. Teflon O-rings are used to eliminate previous problems of swelling encountered with neoprene and viton O-rings.

##### 3. High Temperature Potting Fixture

A bell jar assembly utilizing a heating plate was fabricated to permit potting of metallography samples in a new epoxy resin. A temperature of 80°C is required for proper curing.

##### 4. Floating Head Polishing Fixtures

Two new fixtures were fabricated and installed to improve efficiency in preparing metallographic samples.

#### 5. Fuel Pin Sectioning Saw

Assembly of a new saw was completed as a backup unit for the saw installed in the Disassembly Cell. A new design for a vacuum attachment was installed on the saw to permit more efficient retrieval of dust during sectioning of fuel pins.

#### 6. Sodium Distillation Furnace

The new CVC High Vacuum Pumping Station has been received. Preparations are in process to install the unit in the basement under the Na-Distillation Cell. The thermocouples for the furnace have been calibrated and installed in the UHV feedthrough. Fabrication is now complete with the exception of the power conductor feedthrough. Delivery from the factory has been delayed due to shortages of ceramic material.

#### 7. Electro-Optical Profilometer

Two changes have been made to the profilometer positioning stand to allow operation on severely bowed elements. One prevents the element from disengaging from the centering rollers, and the other change allows the bottom end of the element to "float".

Until recently, the profilometer operator has been able to compensate manually for shifts in fuel element position due to bow, but since many of the fuel elements now being received are severely bowed, we can no longer manually compensate for this correction.

Dual measurements are now provided for all profilometry output data since the bow error is not the same for measurements which are made  $180^\circ$  apart. By subtracting the dual readings from one another ( $0^\circ$  from  $180^\circ$ ,  $45^\circ$  from  $225^\circ$ , etc.) we can easily tell where bow errors occur. Measurements can then be repeated in these areas incrementally to obtain more accurate diameter measurements. This operation is effected by indexing the profilometer to the area in question. When the movement stops, centering is done manually and the fuel element is adjusted until it is vertical; the diameter is then recorded. The fuel element is indexed to a new position and the procedure is repeated.

The incremental method of taking data is very slow even if a large increment (0.5 in.) is used. A maximum of only six readings can be taken per minute. The

automatic mode, in comparison, provides 200 readings/sec. or 12 in./min. The Electronics Design Group at LASL is currently looking into methods for electronically positioning the fuel element. This equipment should allow the automatic processing of a fuel element with any degree of bow, provided the element can be held in the profilometry equipment.

#### 8. Miscellaneous Equipment

A second trunnion fixture for loading the radiography cask has been placed in service. This eliminates the necessity for transferring the fixture between the Wing 9 and DP-West Facilities.

The radiography cart was overhauled. The lead screw shaft end was modified, machined and new drive gears installed with dowel pins for more reliable operation.

Two 50-ton shackles were modified for handling the T-2 casks.

#### B. Inert Atmosphere Systems

(R. W. Basinger, P. A. Mason)

The design of the manipulator through-tube seal package, mentioned in the previous report was improved. Compared to the previous design, an improvement of  $> 50$  times  $\Delta P$  is attainable for a given boot purge flow rate. The design of an assembly for sealing the exterior of the through-tube of the manipulator to the alpha box penetration ports has been completed utilizing an inflatable inner tube. The seal assemblies have been installed in seven manipulators. Three more manipulators are scheduled for modification in the near future.

#### C. Manipulator Maintenance

(W. R. Carter, E. L. Mills, P. A. Mason)

Two mini-manipulators used in the metallography blister were overhauled; one was modified to permit easier installation.

Five AMF manipulators required tape replacement; eleven manipulator boots were replaced.

Four AMF manipulators were modified to permit installation of the new design seal packages which will provide better control of atmosphere and contamination.

#### D. Shipping Casks

(F. J. Fitzgibbon, J. W. Schulte)

Shop modifications have been completed to one of the two LASL vertical casks. Modifications to the second unit will be completed in January 1974. These changes, as reported previously, will permit handling at HFEF north and south facilities.

### III. ANALYTICAL CHEMISTRY

#### A. Gamma Scanning

(J. R. Phillips, T. K. Marshall, J. R. Netuschil, J. N. Quintana)

The precision gamma scanning system has been applied to the nondestructive investigation of the migration properties of selected fission products. Significant differences have been detected in the isotopic distributions of  $^{95}\text{Zr}$  and  $^{95}\text{Nb}$ , of  $^{103}\text{Ru}$  and  $^{106}\text{Ru}$ , and  $^{134}\text{Cs}$  and  $^{137}\text{Cs}$  in irradiated (U,Pu) $\text{O}_2$  fuel pins. Burnup profiles obtained by nondestructive gamma scanning are being correlated with mass spectrometric results.

The principal data processing computer codes for the presentation of gross gamma and isotopic distributions have been converted to the International System (SI) of Units.

#### B. Sealed-Reflux Dissolution System

(J. W. Dahlby, R. R. Geoffrion)

Samples that are difficultly soluble are now dissolved by a sealed-reflux-dissolution technique developed for in-cell use. In this new technique, the sample with 12M HCl and traces of  $\text{HNO}_3$  and HF is contained in a thick-walled, fused-silica tube sealed by closing the top opening with a rubber stopper (Fig. 401-1). The tube is cooled in dry ice to create a partial vacuum, and then heated with a flame approximately 76 mm below the stopper. The walls of the tube are pushed inward by the atmospheric pressure, producing a thick, positive seal capable of withstanding pressures developed in the sealed-reflux or sealed-tube dissolution. The sealed tube is placed in a heating block at  $150^\circ\text{C}$ , Fig. 401-2, until dissolution is complete. The tube is then cooled in dry ice to freeze the sample, scored, broken, and the sample is washed into an appropriate container.

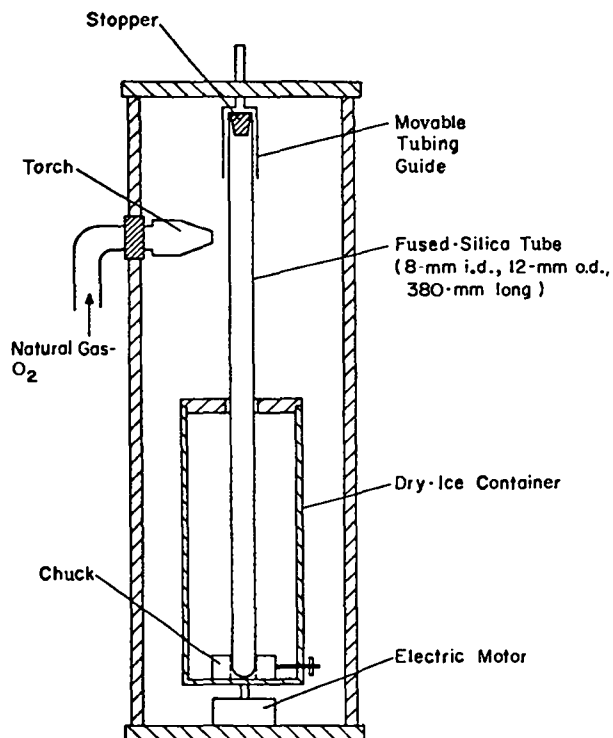


Fig. 401-1. Remote Tube Sealer.

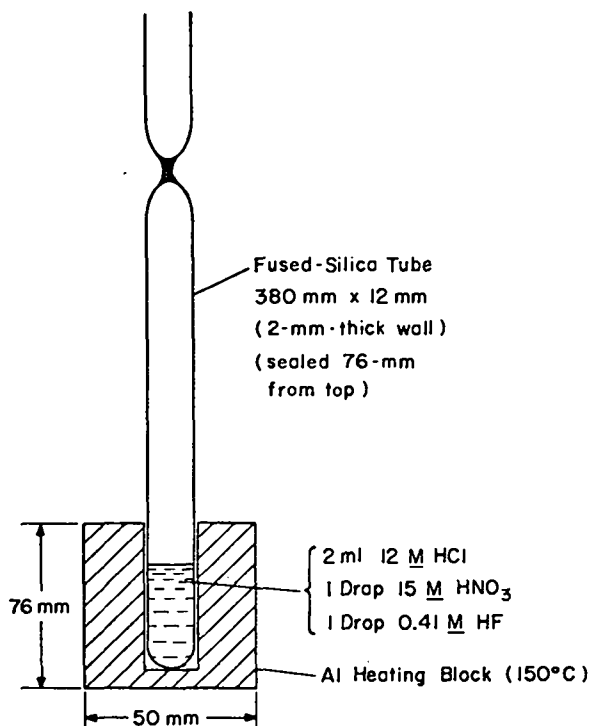


Fig. 401-2. Sealed-Reflux Dissolution System.

When the temperature of the acid solution rises to 150°C, the pressure in the tube is less than 3 MPa (<500 psi), which does not require a compensating external pressure. A metal shell is placed over the tube while the sample is heated to protect the individual tubes in the remote possibility should one of the tubes rupture. The acid refluxes because of a 100°C temperature differential between the top and bottom of the tube. As the system is sealed, the acid is totally contained and the internal pressure prevents the acid from boiling at the elevated temperature. One major advantage of this system is that many tubes can be heated in the block, increasing the total number of samples that can be dissolved simultaneously. Also, if a sample is not dissolved using the sealed-reflux system, the tube can be directly placed in the pressurized sealed-tube dissolution furnace and heated to 300°C and pressurized to 27 MPa.<sup>1</sup> This new sealed-reflux dissolution system has been successfully tested on high-fired thorium oxide. Testing on irradiated material in the hot cell is in progress.

#### IV. MICROSTRUCTURAL ANALYSIS

(J. H. Bender, D. D. Jeffries, K. A. Johnson, J. L. Lehmann, H. D. Lewis)

The photodarkroom trailer now has power and heat. Water supply and drain installation for the trailer are in process.

A new epoxy mounting system has been developed. Its out-of-cell characteristics are very superior giving both good impregnation, good chemical resistance, and excellent metallographic properties. It is in final test stages with respect to high burnup (> 10 at.%) oxide fuel samples. It has given very good impregnation at levels of up to and including 8 at.% burnup on oxide fuels.

#### V. REQUESTS FROM RRD

##### A. Examination of Irradiated Materials

(R. M. Abernathy, K. A. Johnson, M. E. Lazarus, R. A. Morris, J. R. Phillips, J. W. Schulte, G. R. Waterbury, W. F. Zelezny)

During the Second Quarter of FY 1973, twenty-five irradiated fuel capsules were received. The distribution is as follows: GE, 10; HEDL, 15.

Argonne National Laboratory: The scanning electron microscope was used to examine one sample of cladding from each of two irradiated pins.

General Electric Company: Examinations performed on twenty-seven irradiated fuel capsules received on March 21, 1973, April 7, 1973, August 1, 1973, and November 12, 1973 are listed in Table 401-I.

Ten irradiated structural assemblies (L-16 Series) were shipped to ANL-West following nondestructive testing at LASL.

Gulf General Atomic: Eight samples were analyzed for tritium content, and two samples were analyzed for lithium.

Hanford Engineering Development Laboratory: Examinations performed on twenty-four irradiated fuel capsules received on August 1, 1973, August 31, 1973, and November 12, 1973 are listed in Table 401-II.

Two Rover cask inserts were loaned to HEDL to be used for storing irradiated LMFBR pins.

A dried fuel solution from an irradiated pin was sent to HEDL as part of a burnup correlation study.

Los Alamos Scientific Laboratory: Several carbide and nitride fuel pins were examined as part of the technical evaluation being carried out by LASL personnel under the Advanced Fuel Program.

1. BMI Experiments -- Examinations performed on two BMI irradiated fuel capsules received on February 16, 1973 are shown in Table 401-III.

2. LASL Experiments -- Examinations performed on one LASL irradiated fuel capsule received on October 11, 1972 are listed in Table 401-IV.

3. WARD Experiments -- Examinations performed on two irradiated fuel capsules received on February 16, 1973 are listed in Table 401-V.

Density measurements were made on thirteen unirradiated archive cladding samples. Twenty-five measurements were made, three in cell and twenty-two out of cell.

TABLE 401-I

POSTIRRADIATION EXAMINATIONS OF CAPSULES  
AND PINS FROM GE

Examination	No. of Capsules	No. of Pins
1. Visual Inspection	3	17
2. Preliminary Measurements	3	19
3. Profilometry, Optical	--	18
4. Profilometry, Mechanical	--	2
5. Radiography	3	8
6. Na Removal	11	--
7. Clad Removal	11	--
8. Photography, Full Length	3	17
9. Photography, Maximum Bow	3	17
10. Photography, Incremental	2	11
11. Wire Wrap Removal	--	17
12. Photography, Full Length w/o Wire	--	12
13. Photography, Maximum Bow w/o Wire	--	6
14. Photography, Incremental w/o Wire	--	3
15. Eddy Current	3	19
16. Sectioning	--	9
17. Density Measurements	--	6
18. Gamma Scanning ( $^{134}\text{Cs}/^{137}\text{Cs}$ )	1	3
19. Radiochemistry (total $^{134}\text{Cs}$ )	--	2
20. Radiochemistry (total $^{137}\text{Cs}$ )	--	2
21. Total Cs	--	2
22. Shielded Microprobe	--	2 (3 samples)
23. Gamma Scanning <sup>a</sup>	11	--
24. Atom % Burnup	--	3
25. Gas Analysis	17	4
26. Clad Plenum Leach	--	2
27. Density Preparation	--	9 (22 samples)
28. Microstructural Analysis (Optical Microscopy <sup>b</sup> )	--	4 (10 trans. samples) (6 longit. samples)

<sup>a</sup>41 gross gamma scans, 12 complete spectral scans, and 88 isotopic distributions of fission and activation products were determined.

<sup>b</sup>The optical microscopy includes macrophotography, alpha autoradiography, beta-gamma autoradiography, and as-polished and etched photomicroscopy, (including mosaics) in inert (Ar) atmosphere. Specimens from other experimenter's fuel pins, listed in following sections, were examined in like manner.

TABLE 401-II

POST IRRADIATION EXAMINATION OF CAPSULES  
AND PINS FROM HEDL

Examination	No. of Capsules	No. of Pins
1. Visual Examination	--	14
2. Preliminary Measurements	--	21
3. Profilometry, Optical	--	1
4. Radiography	4	10
5. Gamma Scanning <sup>a</sup>	9	--
6. Photography, Full Length	--	14
7. Photography, Maximum Bow	--	14
8. Photography, Incremental	--	13
9. Gas Sampling and Analysis	--	1
10. Eddy Current	--	1
11. Sectioning	--	2
12. Na Melting and Pressurizing Tests	--	1
13. Shielded Microprobe	--	1
14. Atom % Burnup	--	2 (6 samples)
15. Released Fission Gas	--	1 (5 samples)
16. Microstructural Analysis	--	2 (11 trans. samples) (4 longit. samples)

<sup>a</sup>34 gross gamma scans, 13 complete spectral scans, and 92 isotopic distributions of fission and activation products were determined.

TABLE 401-III

POSTIRRADIATION EXAMINATIONS OF BMI  
CAPSULES AND PINS

Examination	No. of Capsules	No. of Pins
1. Na Removal	1	--
2. Clad Removal	1	--
3. Photography, Incremental	--	1
4. Profilometry, Mechanical	--	1
5. Eddy Current	--	1
6. Sectioning	--	1
7. Density Measurements	--	1
8. Atom % Burnup	--	2

TABLE 401-IV  
POSTIRRADIATION EXAMINATIONS OF LASL PINS

<u>Examination</u>	<u>No. of Pins</u>
1. Sectioning	1
2. Shielded Microprobe	1
3. Atom % Burnup	1
4. Microstructural Analysis	4 (13 trans. samples) (3 longit. samples)

TABLE 401-V  
POSTIRRADIATION EXAMINATIONS OF WARD PINS

<u>Examination</u>	<u>No. of Pins</u>
1. Density Measurements	2 (6 samples)
2. Atom % Burnup	2

VI. QUALITY ASSURANCE  
(L. E. Lanham)

A. General

The quality assurance organization has reviewed the HEDL document TC-30 "Postirradiation Examination Requirements for Mixed Oxide Fuel Pins -- PNL-4-40, PNL-4-70, PNL-5-3, PNL-5-15, PNL-7-8, PNL-7-22, and PNL-7-25." The following is a summary of this review.

1. LASL does have a quality assurance program that responds to the requirements of RDT Standard F2-2 for both the destructive and nondestructive examinations requested.
2. Previous examinations have been made and reported to HEDL where all work was under the LASL Quality Assurance Program.
3. Initiating changes in the LASL Quality Assurance Program to the extent requested by HEDL would result in a delay of examinations, would increase the cost of these examinations, and would not bring about an equivalent increase in quality. If there are problem areas, these should be evaluated and appropriate actions taken.

These findings have been discussed with concerned HEDL personnel. As a result of these discussions a visit to LASL has been scheduled in January by HEDL.

An additional person has been added to the quality assurance organization to perform field surveillance of

the examination activities in the 401 Project. The major quality assurance effort has been to establish and implement an independent quality assurance surveillance activity. One man is being used for surveillance activities in Projects 401, 463, and 472.

Corrective actions have been taken on all of the findings of the April 1973 AEC audit. The actions taken have been reported to the AEC.

B. Hot Cell Examinations

A revised traveler document has been prepared to require a technical overcheck of each examination. All new element and pin examinations will be made using the new traveler. This procedure is also being applied to current examinations that were requested on the basis of previous documentation.

An incident was reported on a bent fuel element. An initial review of the incident by both LASL and HEDL indicates there has been no damage to the fuel pin. The preliminary report has been prepared and distributed. Corrective actions have been taken to prevent possible fuel element damage in the unloading operation.

A sequential Betatron radiograph for two adjacent areas was made twice for the same area, but was documented and reported for the adjacent areas in the proper sequence. Position overchecks are made for the area radiographed and the photographic results are overchecked. Although this is the first nonconformance reported for this examination, changes have been initiated for the verification of operations and overcheck of data.

C. Microstructural Analysis

Some problems have been reported in photograph identification. This situation is being investigated. A Specimen Sequential Photographic Log has been initiated to more completely document each photograph. Overchecking procedures are being reviewed.

D. Chemical Analysis

The revised procedures have been issued and are in effect for all chemical analysis under the Quality Assurance Program. All travelers make reference to the new numbers and the new procedure documents are being used.

VII. REFERENCES

1. J. W. Dahlby, G. R. Waterbury, C. D. Montgomery, T. Romanik, "Application of the Sealed-Tube Method to Remote Dissolution of Irradiated Refractory Materials," Proc. 19th Conf. Remote Syst. Technol., p. 191 (1971).

2. T. K. Marshall, J. R. Phillips, B. K. Barnes, G. R. Waterbury, "New Techniques in Two-Dimensional Gamma Scanning," presented at the 17th Conference on Analytical Chemistry in Nuclear Technology, Gatlinburg, TN, October 23-25, 1973.

VIII. PUBLICATIONS

1. C. S. MacDougall, T. K. Marshall, G. M. Matlack, and G. R. Waterbury, "Determination of Oxygen, Hydrogen, and Tritium in Irradiated Reactor Fuels and Cladding Materials," presented at the 17th Conference on Analytical Chemistry in Nuclear Technology, Gatlinburg, TN, October 23-25, 1973

## PROJECT 463

### HIGH PERFORMANCE LMFBR FUEL MATERIALS

Person in Charge: R. D. Baker  
Principal Investigator: J. L. Green

---

#### I. INTRODUCTION

The primary objective of this program is the overall evaluation of the most promising of the candidate fuel systems for advanced LMFBR application. Emphasis currently is placed on the study of the relative merits of stainless steel clad nitride and carbide fuels under conditions that appropriately exploit the potential of these materials to operate to high burnup at high power densities. The major portion of the program is the evaluation of the irradiation performance of these fuel element systems. A continuing series of irradiation experiments is being carried out under steady-state conditions in fast reactor environments to assess the effects of damage and burnup on stainless-steel-clad carbide and nitride fuel elements. These experiments are designed to investigate fuel swelling, interactions between the fuel and clad and thermal bonding medium, fission gas release, and the migration of fuel material and fission products as a function of burnup and irradiation conditions. In addition, experiments are being considered which would allow the study of the effects of rapid, overpower, reactor transients on carbide and nitride fuel assemblies. Contiguous efforts are necessary in the development of fuel material preparation and fabrication procedures as well as the techniques required for the characterization of fuel materials both before and after irradiation.

A second objective in the program is the determination of thermophysical, mechanical and chemical properties and characteristics of plutonium-containing ceramics that are required for their evaluation and use as fuel materials. A broad range of capabilities in this area has

been developed including the study of (1) phase relationships using differential thermal analysis, (2) thermal transport, (3) thermal stability and compatibility, (4) vapor pressure using mass spectrometry, (5) heat content using drop calorimetry, (6) elastic properties using sonic modulus measurements, (7) hot hardness and its temperature dependence, (8) structure and phase relationships using high temperature x-ray and neutron diffraction, (9) thermal expansion, and (10) compressive creep rate as a function of temperature and stress. Several of these techniques are available for use with irradiated fuels.

#### II. IRRADIATION TESTING

The objective of the irradiation testing program is the overall evaluation of the most promising of the candidate fuel systems for advanced LMFBR application. The irradiation experiments are carried out under conditions that take advantage of the potential of these materials to operate to high burnup at high power densities.

##### A. Fuel Synthesis and Fabrication

(K. W. R. Johnson, J. G. Reavis, H. G. Moore, R. W. Walker, C. Baker)

##### 1. Carbide Fuel Production

After a thorough review of the first 225 g batch preparation of  $U_{0.8}Pu_{0.2}C$  synthesized in accordance with a new Quality Assurance procedure, an additional 225 g batch preparation was synthesized. The product of this preparation met all specifications with the exception of the zirconium content. Analysis of the process indicated that in the initial arc-melting process, the repeated

melting of a zirconium button to provide a getter was probably responsible for the high zirconium content of the product.

## 2. Nitride Fuel Development

Previously described scoping experiments<sup>1</sup> were used to evolve a procedure for the preparation of UN or (U,Pu)N pellets for irradiation testing. These experiments also provided a means of testing new equipment and inert recirculating glovebox facilities. The equipment was designed so that it could be used for the synthesis and fabrication of either nitride or carbide pellets. Shown in Table 463-I are some of the experimental parameters along with the product densities from the scoping experiments.

TABLE 463-I

PREPARATION PARAMETERS AND DENSITIES OF UN AND  $U_{0.8}Pu_{0.2}N$  PELLETS

Expt. No.	No. of Hydride Cycles	Decomp. Temp., °C	Sintering Time, h	Sintering Temp., °C	Density % T.D. <sup>a</sup>
UN-3	1	1500	18	2150	92.1
UN-4	3	1340	15	2150	93.8
UN-5	3	1400	16	2150	92.6
UN-6	2	1500	16	2150	92.6
(U,Pu)N-1	2	1100	20	2000	77
(U,Pu)N-2	2	1370	16	2100	87

<sup>a</sup>Based on T.D. = 14.32 g/cm<sup>3</sup>

Although high-density UN pellets were prepared, additional work will be required to produce  $U_{0.8}Pu_{0.2}N$  pellets of comparable density. Microstructural examination of the pellets indicated that they were consistently single phase. In the earlier experiments, it was found that several metallic impurities and the oxygen content of the sintered pellets were quite high. The metallic impurities were found to be related to processing factors. In the initial phase of the preparation, trays fabricated from TZM (titanium, zirconium and molybdenum alloy) were used because they were much easier to fabricate than ones made from pure molybdenum. Sintering on pure molybdenum trays essentially eliminated the Ti and Zr contamination of the sintered pellets. A high tungsten

content gradually diminished to an acceptable level after a break-in period for a WC-lined oscillatory mill jar and ball. Oxygen contamination which initially ranged from 535 to 1100 ppm was reduced to 125 ppm with the establishment of an inert atmosphere in the sintering glovebox.

Listed below is an outline of the nitride preparation procedure evolved from the scoping experiments.

1. Form metal powder by allowing U or U-Pu alloy to react with pure H<sub>2</sub>, then thermally decompose the product hydride (2 cycles required).
2. React the metal powder with N<sub>2</sub> at 650-900°C to form a sesquinitride.
3. Sieve the powder through 170-mesh screen to remove any unreacted metal.
4. Press the powder into large pellets.
5. Heat the pellets in vacuum at 1400°C to form the mononitride.
6. Grind the powder, then sieve through 325 mesh screen.
7. Press the powder into pellets.
8. Heat the pellets in vacuum to 1500°C, then in a nitrogen atmosphere for 8 h at 2200°C. Cool in N<sub>2</sub> to 1500°C, then in vacuum to ambient temperature.
9. Characterize product.

## 3. Equipment Development

The recirculating inert-atmosphere gloveboxes used for nitride preparation and for high-temperature sintering have been put into service and are routinely operating at O<sub>2</sub> and H<sub>2</sub>O concentrations of 0-5 ppm. A new glovebox of the same type is being closed up and will be used for physical inspection and sampling of ceramic fuel materials.

## B. Fuel Element Fabrication

(K. W. R. Johnson, D. G. Clifton, H. E. Strohm, L. L. Marriott)

### 1. Xenon Tagging Device

The calibration of the pressure transducer used in the xenon tagger was completed and the reproducibility of the transducer was found to be satisfactory. The tagging device with the associated feed-throughs for the electrical leads and the gas and vacuum lines was

installed in the weld box and leak tested. Sample containers that have prototypic fuel element plenum volumes were leak checked, cleaned, and are ready for preliminary tagger check-out.

## 2. Centrifuge

A solid, Type 316 stainless steel dummy fuel element was instrumented with three thermocouples and inserted into the centrifuge. The thermocouples were located at points along the element corresponding to the bottom, center, and just above the top of a typical fuel stack. The exterior heaters of the centrifuge were controlled by variable transformers with the centrifuge stationary. Sets of cooling and heating temperatures versus time as a function of the input power to the heaters were measured using a multipoint recorder. These data established the power settings necessary to insure that sodium-bonded fuel elements can be heated and cooled in such a way that the sodium-bond is melted from the top down and frozen from the bottom up.

A rejected sodium-bonded (UPu)N fuel element (C-BMI-5-17) was used in a similar test to determine temperature-versus-time data. These preliminary data indicate that melting and freezing is occurring in a proper sequence. Further experiments will be performed, since these results were for the stationary centrifuge and faster cooling is expected during the actual centrifuging operation.

## 3. Associated Activities

Minor design changes and installations were made in the gloveboxes used for fuel loading, sodium loading, welding, and grinding. One result of these changes has been a decrease in helium consumption to about 25% of the previous rate.

Eddy-current tests of the sodium bonds of the C-5 and O-N1 series fuel elements were completed. The cladding tubing that was sent to Carpenter Technology for ultrasonic overchecking was returned and was found to be acceptable. Fabrication and inspection of components to be used for welding development and qualification were completed. Further documentation of QA procedures for fuel element fabrication is proceeding.

## C. EBR-II Irradiation Testing

(J. O. Barner, J. F. Kerrisk, T. W. Latimer)

The purpose of the EBR-II testing program is the evaluation of the steady-state irradiation behavior of high-performance fuel element systems for application in advanced LMFBR reactors. Several series of carbide- and nitride-fueled experiments have been initiated in the past several years. The main objectives of the irradiations are: (1) the development fuel element designs for use with each fuel type; (2) the determination of the irradiation behavior of the fuel materials; (3) a comparison of sodium and helium bonding; (4) a comparison of different cladding alloys; and (5) the evaluation of the overall irradiation performance of the fuel element systems. The majority of the experiments under test or that have been completed have been encapsulated. Most of the experiments that are currently available for irradiation or that are being designed are singly clad.

### 1. Experiment Description and Status

Fourteen series of experiments have been originated. The description and status of these series are summarized in Tables 463-II to 463-IX. In order to better define the status of those experiments which are undergoing postirradiation examination, the following steps are referenced in the tables:

#### a. Capsule Examination

- a.1 Visual Examination
- a.2 Preliminary Measurements (radiation measurements, etc.)
- a.3 Profilometry
- a.4 Photography
- a.5 Radiography
- a.6 Eddy Current Test
- a.7 Gamma Scan
- a.8 Cover Gas Analysis
- a.9 Deencapsulation

#### b. Element Examination

- b.1 Visual Examination
- b.2 Profilometry
- b.3 Photography
- b.4 Eddy Current Test
- b.5 Fission Gas Analysis

TABLE 463-II

## SERIES K1, K2, AND K3 ENCAPSULATED CARBIDE EXPERIMENTS

Exprmt. No.	Fuel Type <sup>a</sup>	Fuel Density, % Theo.	Bond and Diametral Gap, mm.	Clad Type <sup>b</sup>	Clad O.D. x I.D., mm.	Max. Linear Power, Kw/m <sup>g</sup>	Maximum Centerline Temp., °C <sup>g</sup>	Goal Burnup, at.% <sup>c</sup>	Maximum Current Burnup, at.% <sup>c</sup>	Status
Series K1										
K-36B	MC	90	Na-0.38	SA-316SS	7.62 x 7.11	82 <sup>†</sup>	990 <sup>†</sup>	6	5.85*	b.12 <sup>d</sup>
K-37B	MC	90	Na-0.38	SA-316SS	7.62 x 7.11	85	1000	6	2.9	a.7 <sup>d,e</sup>
K-38B	MC	90	Na-0.38	SA-316SS	7.62 x 7.11	85	1000	6	5.8	a.7 <sup>d,e</sup>
K-39B	MC	90	Na-0.38	SA-316SS	7.62 x 7.11	85	1000	10	5.8	EBR-II, Un-assigned
K-42B	MC	90	Na-0.38	SA-316SS	7.62 x 7.11	85 <sup>†</sup>	1000 <sup>†</sup>	6	4.46*	Completed <sup>f</sup>
Series K2										
K-49	MC	95	Na-0.51	SA-316SS	7.62 x 7.11	130 <sup>†</sup>	1270 <sup>†</sup>	5	3.74*	b.12 <sup>d</sup>
K-50	MC	95	Na-0.51	SA-316SS	7.62 x 7.11	130	1300	6.5	3.6	a.9 <sup>d</sup>
K-51	MC	95	Na-0.51	SA-316SS	7.62 x 7.11	130	1300	8	3.5	a.9 <sup>d</sup>
Series K3										
K-43	MC	94	Na-0.51	SA-316SS	7.62 x 7.11	80	1000	8	5.6	b.3 <sup>d</sup>
K-44	MC	94	Na-0.51	SA-316SS	7.62 x 7.11	80	1000	8	7.1	EBR-II Exam
K-45	MC	94	Na-0.51	SA-316SS	7.62 x 7.11	80	1000	5	2.7	b.9 <sup>d</sup>
K-46	MC	94	Na-0.51	SA-316SS	7.62 x 7.11	80 <sup>†</sup>	965 <sup>†</sup>	5	2.39*	b.12 <sup>d</sup>

<sup>a</sup>M = (U<sub>0.8</sub>Pu<sub>0.2</sub>)

Series 1 and 3 experiments are 93% enriched in <sup>235</sup>U  
Series 2 experiments are 97% enriched in <sup>233</sup>U.

<sup>b</sup>SA = Solution annealed

<sup>c</sup>Burnup values marked with \* were measured using the <sup>148</sup>Nd method. Remaining values were computed from EBR-II data.

<sup>d</sup>Element cladding failure indicated.

<sup>e</sup>Damaged during reconstitution of X152.

<sup>f</sup>Reported in LA-4669-MS

<sup>g</sup>Linear power & centerline temperature marked with † are beginning-of-life values computed using measured burnup results. Remaining values based on EBR-II power adjustment factor of 0.91.

- b. 6 Sectioning
- b. 7 Autoradiography
- b. 8 Metallography
- b. 9 Burnup
- b. 10 Clad Density
- b. 11 Special Tests
- b. 12 Data Reduction
- b. 13 Report Preparation

All hot cell examinations are done by Project 401 personnel under the guidance of Project 463 personnel.

Table 463-II describes the K1, K2, and K3 series tests. In these experiments single-phase, high-purity, uranium-plutonium monocarbide pellets are sodium

bonded to Type 316 stainless steel cladding. In general, the operating linear power ratings of the capsules are relatively high (approximately 85 Kw/m). Three tests at very high power (> 125 Kw/m) were included to determine the effect of high thermal stresses and high fuel temperatures on fuel element behavior. Indications of element cladding failure were found at EBR-II in several experiments from these series (five in subassembly X119B, one from X142, and two from X152), using  $\gamma$ -scanning for <sup>133</sup>Xe. Examinations of these experiments in the LASL hot cells confirmed the failures. Complete postirradiation examination of the failed experiments is continuing.

TABLE 403-III  
SERIES U1300 ENCAPSULATED CARBIDE EXPERIMENTS

Expmnt. No.	Fuel Type <sup>a</sup>	Fuel Density, <sup>b</sup> % Theo.	Bond and Diametral Gap, mm.	Clad Type <sup>d</sup>	Clad O.D. x I.D., mm.	Max. Linear Power, <sup>e</sup> Kw/m <sup>2</sup>	Maximum Centerline Temp., °C	Goal Burnup, at. %	Maximum Current Burnup, at. % <sup>e</sup>	Status
U93	MC+5%M <sub>2</sub> C <sub>3</sub>	86	He-0.10	SA-316SS	7.66 x 6.10	59 <sup>†</sup>	1750	11	9.64 <sup>*</sup>	b.12
U94	MC	85	He-0.18	SA-316SS	7.73 x 6.86	70 <sup>†</sup>	1680	11	9.42 <sup>*</sup>	b.12
U97	MC+5%M <sub>2</sub> C <sub>3</sub>	86	He-0.10	SA-INC-800	7.60 x 6.10	54	1750	11	10.0	b.5
U98	MC+5%M <sub>2</sub> C <sub>3</sub>	86	He-0.18	SA-INC-800	7.60 x 6.86	65	1680	11	9.6	a.7 <sup>f</sup>
U105	MC+5%M <sub>2</sub> C <sub>3</sub>	77	He-0.20	SA-INC-800	7.61 x 6.10	52 <sup>†</sup>	1900	11	9.89 <sup>*</sup>	b.12
U106	MC+5%M <sub>2</sub> C <sub>3</sub>	77	He-0.20	SA-INC-800	7.72 x 6.86	59	1820	11	9.9	a.7 <sup>f</sup>
U110	MC+10%M <sub>2</sub> C <sub>3</sub>	99 <sup>c</sup>	He-0.33	SA-INC-800	7.73 x 6.86	65	1960	10	9.2	a.7
U113	MC+10%M <sub>2</sub> C <sub>3</sub>	98 <sup>c</sup>	He-0.28	SA-INC-800	7.51 x 6.10	50	1880	11	10.2	a.7
U114	MC+15%M <sub>2</sub> C <sub>3</sub>	98 <sup>c</sup>	He-0.18	SA-INC-800	7.72 x 6.86	66	1570	10	9.5	a.7 <sup>f</sup>

<sup>a</sup>M = (U<sub>0.85</sub>Pu<sub>0.15</sub>)

<sup>b</sup>Theoretical density of MC = 13.45 g/cm<sup>3</sup>  
Theoretical density of M<sub>2</sub>C<sub>3</sub> = 12.72 g/cm<sup>3</sup>

<sup>c</sup>Cored pellet with nominal 2.0 mm diameter axial hole

<sup>d</sup>SA = Solution annealed

<sup>e</sup>Burnup values marked with \* were measured using the <sup>148</sup>Nd method. Remaining values were computed from EBR-II data.

<sup>f</sup>Element cladding failure indicated.

<sup>†</sup>Linear power marked with † are beginning-of-life values computed using measured burnup results. Remaining values based on EBR-II power adjustment factor of 0.91.

One unfailed experiment, K-44, recently completed irradiation in subassembly X182 after reaching a maximum burnup of 7.1 at.%. A second unfailed experiment, K-39B, is at EBR-II awaiting further irradiation.

Table 463-III describes the Series U1300 experiments. These experiments contain two-phase, uranium-plutonium carbide fuel pellets which are helium bonded to either Type 316 stainless steel or Incoloy 800 cladding. Two methods for the accommodation of fuel swelling were investigated in this series, i.e., the introduction of internal porosity by the use of either low-density solid fuel pellets or high-density cored pellets. These experiments reached their goal burnup of 10 at.% in subassembly X142 after operation at moderate linear power ratings (approximately 56 Kw/m). Indications of element cladding failure for three experiments were found at EBR-II using  $\gamma$ -scanning for <sup>133</sup>Xe. These element failures have been confirmed by  $\gamma$ -scanning for <sup>137</sup>Cs at LASL. Three of these experiments have completed postirradiation examination and evaluation of the results is currently under way.

Destructive examination of the remaining experiments is awaiting examination of higher priority experiments.

The Series U1950 experiments are described in Table 463-IV. In these experiments, either two-phase or single-phase carbide fuel is helium bonded to Type 304 or 316 stainless steel or to Incoloy 800 cladding. Fuel densities range from 77 to 99% theoretical. These experiments are currently over three-fourths of their goal burnup after operation at low linear power (38 to 44 Kw/m). During interim examination at EBR-II after run 58, <sup>137</sup>Cs was detected by  $\gamma$ -scanning in the sodium reservoir of capsule U136. Release of fission gas from a breached helium-bonded element would be expected. However, no <sup>133</sup>Xe was detected in the capsule plenum. The lack of fission gas in the capsule and the presence of <sup>137</sup>Cs in the capsule sodium present a contradictory picture and the failure of the element in capsule U136 can only be considered tentative and of a low degree. None of the other capsules indicated fuel element failure during the examinations at EBR-II. All 19 capsules were reconstituted

TABLE 463-IV  
SERIES U1950 ENCAPSULATED CARBIDE EXPERIMENTS

Expm't. No.	Fuel Type <sup>b</sup>	Fuel Density, % Theo. <sup>c</sup>	Bond and Diametral Gap, mm.	Clad Type <sup>e</sup>	Clad O. D. x I. D., mm.	Max. Linear Power, Kw/m <sup>g</sup>	Maximum Centerline Temp., °C	Goal Burnup, at. %	Maximum Current Burnup, at. % <sup>g</sup>	Status
U129	MC	86	He-0.41	SA-316SS	7.70 x 6.60	38	1750	11	9.6	EBR-II, X055B
U130	MC	77	He-0.25	SA-316SS	7.70 x 6.60	39	1500	11	9.7	EBR-II, X055B
U131	MC	85	He-0.36	SA-316SS	7.70 x 6.60	38	1490	11	9.4	EBR-II, X055B
U132	MC	85	He-0.36	SA-316SS	7.70 x 6.60	38	1490	11	9.3	EBR-II, X055B
U133	MC	85	He-0.36	SA-316SS	7.70 x 6.60	38	1490	11	9.1	EBR-II, X055B
U134	MC	85	He-0.36	SA-316SS	7.70 x 6.60	38	1490	11	9.2	EBR-II, X055B
U135	MC	85	He-0.36	SA-INC-800	7.67 x 6.60	38	1470	11	9.4	EBR-II, X055B
U136	MC	85	He-0.36	SA-INC-800	7.67 x 6.60	40	1470	11	9.1	EBR-II, X055B <sup>f</sup>
U137	MC+20% M <sub>2</sub> C <sub>3</sub>	97	He-0.36	SA-316SS	7.70 x 6.60	40	1440	10	8.1	EBR-II, X055B
U138A <sup>a</sup>	MC+20% M <sub>2</sub> C <sub>3</sub>	98	He-0.36	SA-316SS	7.44 x 6.60	44	1440	8	5.0	EBR-II, X055B
U139	MC+20% M <sub>2</sub> C <sub>3</sub>	97	He-0.36	SA-INC-800	7.72 x 6.60	44	1440	10	8.2	EBR-II, X055B
U140	MC	90	He-0.36	SA-INC-800	7.72 x 6.60	41	1460	10	8.8	EBR-II, X055B
U141	MC	91	He-0.25	SA-316SS	7.70 x 6.60	43	1460	10	8.6	EBR-II, X055B
U142	MC	91	He-0.25	SA-316SS	7.72 x 6.60	43	1460	11	8.7	EBR-II, X055B
U143	MC+20% M <sub>2</sub> C <sub>3</sub>	96 <sup>d</sup>	He-0.36	SA-INC-800	7.67 x 6.60	38	1390	11	8.9	EBR-II, X055B
U144	MC+20% M <sub>2</sub> C <sub>3</sub>	96 <sup>d</sup>	He-0.36	SA-316SS	7.72 x 6.60	39	1390	11	9.0	EBR-II, X055B
U145	MC	90	Na-0.76	SA-304SS	7.75 x 6.86	40	820	10	8.5	EBR-II, X055B
U146A <sup>a</sup>	MC+20% M <sub>2</sub> C <sub>3</sub>	99	Na-0.76	SA-304SS	7.62 x 6.86	41	810	8	4.9	EBR-II, X055B
U147	MC+20% M <sub>2</sub> C <sub>3</sub>	97	Na-0.76	SA-INC-800	7.72 x 6.86	42	810	10	8.6	EBR-II, X055B

<sup>a</sup>Capsules 138 and 146 were removed at 4.5 at. % burnup for TREAT testing. Duplicates replaced the originals.

<sup>b</sup>M = (U<sub>0.85</sub>Pu<sub>0.15</sub>); U is 60% enriched in <sup>235</sup>U.

<sup>c</sup>Theoretical density of MC = 13.49 g/cm<sup>3</sup>  
Theoretical density of M<sub>2</sub>C<sub>3</sub> = 12.76 g/cm<sup>3</sup>

<sup>d</sup>Cored pellet with nominal 2.0 mm diameter axial hole.

<sup>e</sup>SA = Solution annealed.

<sup>f</sup>Possible element cladding failure indicated.

<sup>g</sup>Computed using EBR-II power adjustment factor of 0.91.

into subassembly X055B which is currently being irradiated.

The Series U1930 and U1960 experiments are described in Table 463-V. Experimental parameters include fuel type, fuel density, bond type, and cladding type. The operating linear power ratings for the experiments are relatively high (73-100 Kw/m). Nondestructive examination of the eleven experiments listed in part A of Table 463-V was completed several months ago. The results of these examinations showed that fuel

elements U194 and U200 had failed. Destructive examination of this group of experiments has been completed. Data reduction and interpretation are continuing.

The experiments listed in part B of Table 463-V recently completed irradiation in subassembly X182. Prior to the irradiation in X182 elements U188, U190, U193, and U196 had not failed after maximum burnups of 8.5 at. % and elements U199, U201, U207, and U209 had not failed after maximum burnups of 5.5 at. %. After an accumulation of approximately an additional 2 at. % burnup, elements

TABLE 4(3-V)  
SERIES U1930 AND U1960 ENCAPSULATED CARBIDE EXPERIMENTS

Expmt. No.	Fuel Type <sup>a</sup>	Fuel Density, % Theo. <sup>b</sup>	Bond and Diametral Gap, mm.	Clad Type <sup>d</sup>	Clad O. D. x I. D., mm.	Max. Linear Power, Kw/m <sup>2</sup> <sup>b</sup>	Maximum Centerline Temp., °C <sup>h</sup>	Goal Burnup, at. %	Maximum Current Burnup, at. % <sup>g</sup>	Status
U187	MC+5%M <sub>2</sub> C <sub>3</sub>	86	He-0.18	SA-316SS	7.72 x 6.60	77 <sup>†</sup>	1930	5	4.60*	b.12
U189	MC+5%M <sub>2</sub> C <sub>3</sub>	85	He-0.25	SA-INC-800	7.67 x 6.60	81 <sup>†</sup>	1930	5	4.80*	b.12
U191	MC	92	Na-0.76	SA-304SS	7.72 x 6.91	84 <sup>†</sup>	1010 <sup>†</sup>	5	4.50*	b.12
U192	MC	92	Na-0.76	SA-304SS	7.75 x 6.91	73 <sup>†</sup>	940 <sup>†</sup>	5	4.3	b.12
U194	MC+10%M <sub>2</sub> C <sub>3</sub>	98	Na-0.84	SA-304SS	7.75 x 6.91	81 <sup>†</sup>	980 <sup>†</sup>	5	4.64*	b.12 <sup>e</sup>
U195	MC+10%M <sub>2</sub> C <sub>3</sub>	98	Na-0.84	SA-304SS	7.75 x 6.91	83 <sup>†</sup>	990 <sup>†</sup>	5	4.94*	b.12
U197	MC+10%M <sub>2</sub> C <sub>3</sub>	98	Na-0.84	SA-INC-800	7.75 x 6.91	80 <sup>†</sup>	1020 <sup>†</sup>	5	4.90*	b.12
U198	MC+10%M <sub>2</sub> C <sub>3</sub>	98	Na-0.84	SA-INC-800	7.75 x 6.91	84 <sup>†</sup>	1000 <sup>†</sup>	5	4.78*	b.12
U200	MC+5%M <sub>2</sub> C <sub>3</sub>	86	He-0.23	SA-304SS	7.32 x 6.60	83 <sup>†</sup>	2040	5	4.72*	b.12 <sup>e</sup>
U206	MC+5%M <sub>2</sub> C <sub>3</sub>	90	He-0.25	SA-316SS	7.44 x 6.58	90 <sup>†</sup>	2080	5	4.96*	b.12
U208	MC+10%M <sub>2</sub> C <sub>3</sub>	97 <sup>c</sup>	He-0.30	SA-316SS	7.44 x 6.58	87 <sup>†</sup>	1910	5	5.00*	b.12
F										
U188	MC+5%M <sub>2</sub> C <sub>3</sub>	85	He-0.18	SA-316SS	7.72 x 6.60	90	1930	11	11.0	EBR-II, Exam, <sup>c</sup>
U190	MC+5%M <sub>2</sub> C <sub>3</sub>	85	He-0.28	SA-INC-800	7.37 x 6.60	90	1930	11	11.0	EBR-II, Exam,
U193	MC	92	Na-0.79	SA-304SS	7.75 x 6.91	94	1000	11	11.0	EBR-II, Exam, <sup>e</sup>
U196	MC+15%M <sub>2</sub> C <sub>3</sub>	98	Na-0.79	SA-304SS	7.75 x 6.91	97	1000	11	10.9	EBR-II, Exam, <sup>e</sup>
U199	MC+10%M <sub>2</sub> C <sub>3</sub>	98	Na-0.79	SA-INC-800	7.75 x 6.91	100	1000	11	8.2	EBR-II, Exam,
U201	MC+5%M <sub>2</sub> C <sub>3</sub>	85	He-0.23	SA-304SS	7.32 x 6.60	90	2040	11	7.8	EBR-II, Exam, <sup>e</sup>
U207	MC+5%M <sub>2</sub> C <sub>3</sub>	90	He-0.25	SA-316SS	7.44 x 6.58	94	2090	11	7.9	EBR-II, Exam, <sup>c</sup>
U209	MC+10%M <sub>2</sub> C <sub>3</sub>	97 <sup>c</sup>	He-0.30	SA-316SS	7.44 x 6.58	92	1910	11	7.9	EBR-II, Exam, <sup>e</sup>
C										
U185	MC+10%M <sub>2</sub> C <sub>3</sub>	97	He-0.28	SA-316SS	7.72 x 6.60	90	2190	3	2.7	a.7
U186	MC+10%M <sub>2</sub> C <sub>3</sub>	97	He-0.28	SA-316SS	7.72 x 6.60	90	2190	3	2.7	a.7
U202	MC+5%M <sub>2</sub> C <sub>3</sub>	85	He-0	SA-316SS	6.83 x 6.38	94	1270	3	2.5	a.7
U203	MC+5%M <sub>2</sub> C <sub>3</sub>	85	He-0.05	SA-316SS	7.32 x 6.43	93	1260	3	2.5	a.7
U204	MC+10%M <sub>2</sub> C <sub>3</sub>	97 <sup>c</sup>	He-0.05	SA-316SS	6.76 x 6.32	96	1130	3	2.6	a.7
U205	MC+10%M <sub>2</sub> C <sub>3</sub>	97 <sup>c</sup>	He-0.08	SA-316SS	7.21 x 6.35	95	1120	3	2.6	a.7
D										
U260	MC+10%M <sub>2</sub> C <sub>3</sub>	98	He-0.48	20CW-316SS	7.67 x 6.71	102	2590	12	0	EBR-II, unassigned
U261	MC+10%M <sub>2</sub> C <sub>3</sub>	98	He-0.38	SA-316SS	7.49 x 6.60	102	2590	12	0	EBR-II, unassigned <sup>f</sup>
U262	MC+10%M <sub>2</sub> C <sub>3</sub>	96	He-0.38	SA-INC-800	7.34 x 6.60	102	2590	12	0	EBR-II, unassigned

<sup>a</sup>M = (U<sub>0.85</sub>Pu<sub>0.15</sub>)

<sup>b</sup>Theoretical density of MC = 13.45 g/cm<sup>3</sup>  
Theoretical density of M<sub>2</sub>C<sub>3</sub> = 12.72 g/cm<sup>3</sup>

<sup>c</sup>Cored pellet with nominal 2.0 mm diametral axial hole.

<sup>d</sup>SA = Solution annealed; 20 CW = 20% cold worked.

<sup>e</sup>Element cladding failure.

<sup>f</sup>EBR-II eddy current test indicates capsule bond discontinuity.

<sup>g</sup>Burnup values marked with \* were measured using the <sup>148</sup>Nd method. Remaining values were computed using an EBR-II power adjustment factor of 0.91.

<sup>h</sup>Linear power and centerline temperature marked with <sup>†</sup> are beginning-of-life values computed using the measured burnup results. Remaining values are based in EBR-II power adjustment factor of 0.91.

U190 and U199 have not failed. However, U188, U193, U196, U201, U207, and U209 have failed as evidenced by  $\gamma$ -scanning at EBR-II. All of the experiments in this group will be returned to LASL for examination.

The experiments listed in part C of Table 463-V were used as replacement capsules in order to allow the irradiation to be continued to the desired burnup in lead experiments from other series. Only a cursory postirradiation is planned for these elements. Nondestructive

TABLE 463-VI  
SERIES WF ENCAPSULATED CARBIDE EXPERIMENTS

Expt. No.	Fuel Type <sup>a</sup>	Fuel Density, % Theo. <sup>b</sup>	Bond and Diametral Gap, mm.	Clad Type <sup>c</sup>	Clad O. D. x I. D., mm.	Max. Linear Power, Kw/m <sup>f</sup>	Maximum Centerline Temp., °C.	Goal Burnup, at. %	Maximum Current Burnup, at. % <sup>e</sup>	Status
W3F	MC+15%M <sub>2</sub> C <sub>3</sub>	93	Na-0.64	SA-316SS	7.62 x 7.01	81	1000	10	5.5	EBR-II, unassigned
W4F	MC+10%M <sub>2</sub> C <sub>3</sub>	95	Na-0.69	SA-316SS	7.62 x 7.01	82 <sup>†</sup>	950	6	5.32*	b. 12
W5F	MC+10%M <sub>2</sub> C <sub>3</sub>	91	Na-0.25	SA-316SS	6.35 x 5.84	60	925	10	5.4	EBR-II, Exam.
W6F	MC+10%M <sub>2</sub> C <sub>3</sub>	90	Na-0.28	SA-316SS	6.38 x 5.87	60	925	6	5.4	EBR-II, Exam. <sup>d</sup>
W7F	MC+5%M <sub>2</sub> C <sub>3</sub>	90	Na-0.69	20CW-316SS	7.62 x 7.01	81	1000	10	5.5	EBR-II, unassigned
W8F	MC+5%M <sub>2</sub> C <sub>3</sub>	94	Na-0.64	20CW-316SS	7.62 x 7.01	83 <sup>†</sup>	950	6	5.82*	b. 12
W10F	MC	89	Na-0.30	SA-316SS	6.38 x 5.87	60	925	10	5.4	EBR-II, unassigned
W12F	MC+25%M <sub>2</sub> C <sub>3</sub>	97	Na-0.33	SA-316SS	6.38 x 5.87	63	975	10	5.4	EBR-II, Exam.

<sup>a</sup>M = (U<sub>0.8</sub>Pu<sub>0.2</sub>)

<sup>b</sup>Theoretical density of MC = 13.45 g/cm<sup>3</sup>  
Theoretical density of M<sub>2</sub>C<sub>3</sub> = 12.72 g/cm<sup>3</sup>

<sup>c</sup>SA = Solution annealed, 20 CW = 20% cold worked.

<sup>d</sup>Element cladding failure indicated by gamma scanning.

<sup>e</sup>Burnup values marked with \* were measured using the <sup>148</sup>Nd method. Remaining values were computed using EBR-II power adjustment factor of 0.91.

<sup>f</sup>Linear power marked with † are beginning-of-life values computed using the measured burnup results. Remaining values are based on EBR-II power adjustment factor of 0.91.

examination of the experiment is complete. The experiments listed in part D of Table 463-V are awaiting insertion into the reactor. Capsule U261 will be returned to LASL for rework of an apparent sodium bond defect in the capsule-element annulus.

Table 463-VI describes the Series WF experiments. These sodium-bonded, carbide capsules were designed to evaluate the effects of (1) various amounts of sesquicarbide in the fuel, (2) linear power rating, and (3) cladding cold work on element performance. The amount of sesquicarbide reported to be in the fuel varies from 0 to 24 vol%. Recently one experiment, W6F, was determined to have an element cladding failure after a maximum burnup of 5.4 at. %. This is the first failure in this series and was determined by  $\gamma$ -scanning at EBR-II. W6F will be returned to LASL for examination. Two other experiments, W4F and W8F, have completed postirradiation examination and evaluation of the results is under way. Irradiation of the remaining five capsules will continue

to a goal burnup of 10 at. %.

Table 463-VII describes the Series B-1, B-2, and B-3 experiments. These capsules are fueled with single-phase, uranium-plutonium mononitride. All the elements in Series B-1 and B-2 are sodium bonded and clad with either Type 304 or 316 welded stainless steel tubing. Operating linear power ratings for the experiments are relatively high (79-118 Kw/m). Capsules B-1-4 and B-2-5 have been examined using  $\gamma$ -scanning techniques for the detection of <sup>137</sup>Cs, and both elements are apparently intact. Further irradiation of these two capsules is planned. The remaining experiments from these series were removed from subassembly X152. During the interim examination, capsules B-1-1, B-1-2, B-2-2, B-2-6, and B-2-7, were found to have failed as indicated by  $\gamma$ -scanning for <sup>133</sup>Xe at EBR-II. The elements in capsules B-2-1 and B-2-3 were found to be intact. Capsule B-2-3 recently completed irradiation in subassembly X182. It is unfailed after a maximum burnup of 8.5 at. % burnup,

TABLE 463-VII  
 SERIES B-1, B-2 AND B-3 ENCAPSULATED NITRIDE EXPERIMENTS

Expm't. No.	Fuel Type <sup>a</sup>	Fuel Density, % Theo. <sup>b</sup>	Bond and Diametral Gap, mm.	Clad Type <sup>d</sup>	Clad O.D. x I.D., mm.	Max. Linear Power, Kw/m <sup>h</sup>	Maximum Centerline Temp., °C <sup>h</sup>	Goal Burnup, at.%	Maximum Current Burnup, at.% <sup>e</sup>	Status
-----Series B-1-----										
B-1-1	MN	94	Na-0.48	SA-304SS	7.37 x 6.35	79 <sup>†</sup>	1045 <sup>†</sup>	5	5.70*	b.12 <sup>f</sup>
B-1-2	MN	94	Na-0.46	SA-304SS	7.37 x 6.35	81	1100	9	5.7	a.7
B-1-4	MN	94	Na-0.30	SA-304SS	7.37 x 6.35	85	1100	10	2.7	LASL, unassigned <sup>g</sup>
-----Series B-2-----										
B-2-1	MN	95	Na-0.53	SA-316SS	8.02 x 6.99	98	1230	10	5.7	EBR-II, unassigned
B-2-2	MN	94	Na-0.51	SA-316SS	8.01 x 6.98	93 <sup>†</sup>	1230	9	5.46*	b.12 <sup>f</sup>
B-2-3	MN	94	Na-0.51	SA-316SS	8.00 x 6.99	97	1230	12	8.5	EBR-II, Exam.
B-2-5	MN	94	Na-0.71	SA-316SS	8.00 x 7.21	97	1230	12	2.7	LASL, unassigned <sup>g</sup>
B-2-6	MN	94	Na-0.53	SA-316SS	8.03 x 7.49	109	1230	6	5.6	a.7 <sup>f</sup>
B-2-7	MN	94	Na-0.51	SA-316SS	8.03 x 7.49	110	1230	12	5.6	a.7 <sup>f</sup>
-----Series B-3-----										
B-3-2	MN	88	Na-0.23	SA-316SS	8.01 x 7.22	110 <sup>†</sup>	1235 <sup>†</sup>	9	2.78*	b.12 <sup>f</sup>
B-3-3	MN	91	Na-0.25	SA-316SS	8.01 x 7.22	116	1280	12	2.8	a.7 <sup>f</sup>
B-3-4	MN	94	Na-0.33	SA-316SS	8.01 x 7.22	108 <sup>†</sup>	1200 <sup>†</sup>	12	2.70*	b.12 <sup>f</sup>
B-3-5	MN	90	Na-0.25	SA-316SS	8.01 x 7.48	118 <sup>†</sup>	1255 <sup>†</sup>	6	2.74*	b.12 <sup>f</sup>
B-3-6	MN	95 <sup>c</sup>	He-0.13	SA-316SS	8.00 x 6.99	102	1920	10	6.0	EBR-II, Exam.
B-3-7	MN	89	He-0.13	SA-316SS	8.00 x 6.99	102	1920	6	6.0	EBR-II, Exam.
B-3-8	MN	90 <sup>c</sup>	He-0.13	SA-316SS	8.00 x 6.99	97	1870	10	6.0	EBR-II, Exam.

<sup>a</sup>M = (U<sub>0.8</sub>Pu<sub>0.2</sub>)

<sup>b</sup>Theoretical density of MN = 14.17 g/cm<sup>3</sup>

<sup>c</sup>Cored pellet with nominal 1.78 mm. diameter axial hole.

<sup>d</sup>Cladding is welded tubing  
 SA = Solution annealed

<sup>e</sup>Burnup values marked with \* were measured using the <sup>148</sup>Nd method. Remaining values were computed using an EBR-II power adjustment factor of 0.91.

<sup>f</sup>Element cladding failure indicated.

<sup>g</sup>Available for further irradiation.

<sup>h</sup>Linear power and centerline temperature marked with † are beginning-of-life values computed using measured burnup results. Remaining values based on EBR-II power adjustment factor of 0.91.

Further irradiation is planned. Destructive examination of B-1-1 and B-2-2 is currently under way. Examination of the remaining experiments that are available is pending examination of higher priority capsules.

Series B-3 is similar to the B-1 and B-2 series except that three helium-bonded experiments are included and the average operating linear power ratings are slightly higher. The three helium-bonded elements have not failed at a maximum burnup of 6 at.%. Helium-bonded experiment B-3-7 will be returned to LASL for destructive examination. The other two helium-bonded experiments will continue irradiation.

Three of the failed sodium-bonded elements in the Series B-3 have completed postirradiation examination. The fourth experiment of this type is awaiting examination pending examination of higher priority experiments.

The Series U5100 singly-clad experiments are described in Table 463-VIII. In this group, either single-phase or two-phase carbide fuel is sodium bonded to Type 304 or 316 stainless steel or to Incoloy 800. In seven of the elements, a perforated shroud is incorporated primarily to test the retention of fuel fragments by close-fitting tubes. A secondary objective of the shroud is to study the effectiveness of the shroud alloy as a carbon getter.

TABLE 463-VIII  
 SERIES U5100 SINGLY CLAD CARBIDE EXPERIMENTS

Expt. No.	Fuel Type <sup>a</sup>	Fuel Density, % Theo. <sup>b</sup>	Bond and Diametral Gap, mm. <sup>c</sup>	Clad Type <sup>d</sup>	Clad O. D. x I. D., mm.	Max. Linear Power, Kw/m <sup>f</sup>	Maximum Centerline Temp., °C	Goal Burnup, at. %	Maximum Current Burnup, at. % <sup>i</sup>	Status <sup>e</sup>
U241	MC	94	Na-0.46	SA-304SS	7.87 x 7.14	107	1170	6	3.0	EBR-II, X156
U242	MC	93	Na-0.44	SA-304SS	7.87 x 7.14	107	1170	9	3.0	EBR-II, X156
U243	MC	93	Na-0.80	SA-304SS	7.87 x 7.14	101	1150	6	2.9	EBR-II, X156
U244	MC	93	Na-0.44	SA-304SS	7.87 x 7.14	107	1170	9	3.0	EBR-II, X156
U245	MC	93	Na-0.81	SA-304SS	7.87 x 7.14	101	1150	12	2.9	EBR-II, X156
U246	MC	93	Na-0.43	SA-316SS	7.87 x 7.14	109	1190	6	3.1	EBR-II, X156
U247	MC	93	Na-0.81	SA-316SS	7.87 x 7.14	101	1150	6	2.9	EBR-II, X156
U248	MC	93	Na-0.81	SA-316SS	7.87 x 7.14	109	1140	12	3.1	EBR-II, X156
U249	MC	93	Na-0.43	SA-INC-800	7.85 x 7.14	109	1210	6	3.1	EBR-II, X156
U250	MC	93	Na-0.81	SA-INC-800	7.85 x 7.14	109	1140	6	3.1	EBR-II, X156
U251	MC	93	Na-0.81	SA-304SS	7.87 x 7.14	109	1140	12	3.1	EBR-II, X156
U252	MC	93	Na-0.64	SA-304SS	7.87 x 7.14	109	1140	12	3.1	EBR-II, X156
U253	MC	93	Na-0.66	SA-304SS	7.87 x 7.14	101	1140	12	2.9	EBR-II, X156
U254	MC	93	Na-0.66	SA-304SS	7.87 x 7.14	101	1140	12	2.9	EBR-II, X156
U256	MC+15%M <sub>2</sub> C <sub>3</sub>	96	Na-0.61	SA-304SS	7.85 x 7.14	101	1140	12	2.9	EBR-II, X156
U257	MC+15%M <sub>2</sub> C <sub>3</sub>	96	Na-0.58	SA-INC-800	7.85 x 7.14	100	1130	12	2.9	EBR-II, X156
U258	MC+15%M <sub>2</sub> C <sub>3</sub>	96	Na-0.58	SA-304SS	7.87 x 7.14	100	1140	6	2.9	EBR-II, X156
U259	MC+15%M <sub>2</sub> C <sub>3</sub>	96	Na-0.58	SA-INC-800	7.85 x 7.14	103	1150	12	3.0	EBR-II, X156

<sup>a</sup>M = (U<sub>0.85</sub>Pu<sub>0.15</sub>)

<sup>b</sup>Theoretical density of MC = 13.45 g/cm<sup>3</sup>  
 Theoretical density of M<sub>2</sub>C<sub>3</sub> = 12.72 g/cm<sup>3</sup>

<sup>c</sup>Elements U252 through U259 contain slotted shroud tubes ~ 0.09 mm thick, made of V, Fe, 304SS, V, Ta, 304SS, and 304SS, respectively. The shroud thickness is not included in the bond gap value.

<sup>d</sup>SA = Solution annealed

<sup>e</sup>Element cladding failure indicated in subassembly

<sup>f</sup>Computed using an EBR-II power adjustment factor of 0.91.

These experiments are being irradiated in subassembly X156. An element failure has been indicated in this subassembly after a maximum burnup of 3 at.%. The interpretation of results from EBR-II reactor monitoring systems is that the size of the failure is very small. The subassembly was removed from the reactor on January 1, 1974. In order to prevent damage to the unfailed experiments during ex-reactor handling, a cooling time of 70 days will be required to reduce element surface temperatures to levels where a minimum of caustic corrosion can be assured. Weight and neutron radiographic examinations will be made at HFEF in order to determine the failed element. This element will be returned to LASL for destructive examination. It is planned to continue irradiation of the remaining elements.

The C-5 and O-N1 series of singly-clad experiments are described in Table 463-IX. Single-phase nitride fuel is sodium bonded to 20% cold-worked Type 316 stainless steel cladding in all of the fuel elements in this group. Profilometry measurements of the C-5 series elements have been made using the same equipment that will be used for the postirradiation examination. Shipment of selected elements to EBR-II is pending LASL review of the experiments from a quality assurance standpoint.

The O-N1 series of singly-clad experiments is similar to the C-5 series. The elements are fueled with (U<sub>0.8</sub>Pu<sub>0.2</sub>)N which is sodium bonded to 20% cold-worked Type 316 stainless steel cladding. Three elements have been rejected because of large fuel chips in the sodium

TABLE 463-IX  
SERIES C-5 AND O-N1 SINGLY CLAD NITRIDE EXPERIMENTS

Expmnt. No.	Fuel Type <sup>a</sup>	Fuel Density, % Theo. <sup>b</sup>	Bond and Diametral Gap, mm.	Clad Type <sup>c</sup>	Clad O.D. x I.D., mm.	Max. Linear Power, Kw/m	Maximum Centerline Temp., °C	Goal Burnup, at. %	Maximum Current Burnup, at. %	Status
C-5-1	MN	93	Na-0.51	20CW-316SS	7.87 x 7.11	---	---	---	---	Reject <sup>d,e</sup>
C-5-2	MN	94	Na-0.51	20CW-316SS	7.87 x 7.11	---	---	---	---	Reject <sup>d,e</sup>
C-5-3	MN	95	Na-0.51	20CW-316SS	7.87 x 7.11	---	---	---	---	Reject <sup>d,e</sup>
C-5-4	MN	96	Na-0.53	20CW-316SS	7.87 x 7.11	109	1160	12	0	At LASL <sup>g</sup>
C-5-5	MN	96	Na-0.51	20CW-316SS	7.87 x 7.11	---	---	---	---	Reject <sup>f</sup>
C-5-6	MN	94	Na-0.53	20CW-316SS	7.87 x 7.11	109	1160	12	0	At LASL <sup>g</sup>
C-5-7	MN	95	Na-0.51	20CW-316SS	7.87 x 7.11	111	1180	12	0	At LASL <sup>g</sup>
C-5-8	MN	95	Na-0.76	20CW-316SS	7.87 x 7.11	107	1130	12	0	At LASL <sup>g</sup>
C-5-9	MN	95	Na-0.51	20CW-316SS	7.87 x 7.11	110	1130	12	0	At LASL <sup>g</sup>
C-5-10	MN	95	Na-0.51	20CW-316SS	7.87 x 7.11	107	1100	12	0	At LASL <sup>g</sup>
C-5-11	MN	95	Na-0.51	20CW-316SS	7.87 x 7.11	110	1120	12	0	At LASL <sup>g</sup>
C-5-12	MN	95	Na-0.76	20CW-316SS	7.87 x 7.11	107	1120	12	0	At LASL <sup>g</sup>
C-5-13	MN	96	Na-0.76	20CW-316SS	7.87 x 7.11	105	1110	12	0	At LASL <sup>g</sup>
C-5-14	MN	97	Na-0.76	20CW-316SS	7.87 x 7.11	105	1140	12	0	At LASL <sup>g</sup>
C-5-15	MN	96	Na-0.76	20CW-316SS	7.87 x 7.11	105	1110	12	0	At LASL <sup>g</sup>
C-5-16	MN	96	Na-0.76	20CW-316SS	7.87 x 7.11	107	1120	12	0	At LASL <sup>g</sup>
C-5-17	MN	97	Na-0.76	20CW-316SS	7.87 x 7.11	---	---	---	---	Reject <sup>e</sup>
C-5-18	MN	95	Na-0.53	20CW-316SS	7.87 x 7.11	107	1110	12	0	At LASL <sup>g</sup>
C-5-19	MN	94	Na-0.53	20CW-316SS	7.87 x 7.11	108	1120	12	0	At LASL <sup>g</sup>
C-5-20	MN	96	Na-0.53	20CW-316SS	7.87 x 7.11	106	1110	12	0	At LASL <sup>g</sup>
O-N1-1	MN	91	Na-0.51	20CW-316SS	7.87 x 7.11	108	1140	12	0	At LASL <sup>g</sup>
O-N1-2	MN	91	Na-0.51	20CW-316SS	7.87 x 7.11	---	---	---	---	Reject <sup>d</sup>
O-N1-3	MN	91	Na-0.51	20CW-316SS	7.87 x 7.11	107	1160	12	0	At LASL <sup>g</sup>
O-N1-4	MN	90	Na-0.51	20CW-316SS	7.87 x 7.11	108	1160	12	0	At LASL <sup>g</sup>
O-N1-5	MN	91	Na-0.51	20CW-316SS	7.87 x 7.11	---	---	---	---	Reject <sup>d</sup>
O-N1-6	MN	90	Na-0.51	20CW-316SS	7.87 x 7.11	---	---	---	---	Reject <sup>d</sup>
O-N1-8	MN	91	Na-0.51	20CW-316SS	7.87 x 7.11	109	1120	12	0	At LASL <sup>g</sup>

<sup>a</sup>M = (U<sub>0.8</sub>Pu<sub>0.2</sub>)

<sup>e</sup>Air in plenum

<sup>b</sup>Theoretical density of MN = 14.17 g/cm<sup>3</sup>

<sup>f</sup>Possible impurities present

<sup>c</sup>20CW = 20% cold worked

<sup>g</sup>QA evaluation in progress

<sup>d</sup>Fuel chips in bond

annulus. The diameters of the elements have been measured on the same profilometer that will be used after irradiation. Eddy current examination of these elements indicates multiple sodium bond defects. All elements will be rebonded. It is planned that four of the fuel elements from Series O-N1 will be irradiated with selected elements from Series C-5.

In addition to the experiments described above, two nitride-fueled thermal irradiation experiments from ORNL (43N1 and 43N2) will be examined. Results and status will be reported in future reports.

A series of singly-clad elements is currently being designed to irradiate sodium-bonded carbide and nitride fuels under, as nearly as possible, identical conditions.

## 2. Postirradiation Examination Results

As indicated in the previous section, most of the elements undergoing postirradiation examination are in the intermediate stages of their examination. As a compromise between reporting piecemeal results on all elements as they are obtained and waiting for complete results on a related series of experiments before reporting, this section will report significant trends in examination results as they become apparent. These trends should be considered as preliminary, since additional examination results may alter initial ideas. Final examination results will be reported in topical reports.

### Gas Bubbles in the Fuel Element Sodium Bond:

One of the advantages of sodium bonded high-performance fuel elements is the high thermal conductivity of the bond, which reduces fuel temperatures, and thus fuel swelling, at high power density. If gas bubbles exist in the fuel element sodium bond, the heat flux through the bubbles will be severely restricted, since the thermal conductivity of the gas is much lower (about an order of magnitude) than that of liquid sodium. Heat which would normally flow through the bubble area will be redistributed to flow through adjacent areas where a liquid sodium bond remains. The net result of a gas bubble in the sodium bond will be higher fuel temperatures under the bubble and a higher clad heat flux in the sodium-bonded region adjacent to the bubble.

Gas bubbles can exist in a fuel element sodium bond at fabrication or they could result from the release of fission gas from the fuel to the bond during irradiation. Bond bubbles or voids present after fabrication can be detected using eddy current measurements. Current technology allows voids or bubbles greater than 2 mm in diameter to be easily detected. If voids are indicated in a completed fuel element, the element can be rebonded until no voids or bubbles are detected, or rejected if they cannot be eliminated. Thus the size of gas bubbles in the sodium bond can be limited in new fuel elements.

During irradiation, fission gas (Kr and Xe) is generated in the fuel. For a typical fuel element with 8 mm o.d. cladding, the fuel will generate about  $70 \text{ mm}^3$  (STP) of fission gas per mm of fuel length for one at.% burnup.

For a 0.5 mm diametral sodium bond, the bond volume is about  $5 \text{ mm}^3$  per mm of fuel length. Even with the low fission gas release observed with sodium-bonded carbides (e.g., 5%), enough fission gas is released within a few atom percent burnup to completely fill the sodium-bond volume. Thus if a mechanism is available to retain fission gas in the sodium bond, gas bubbles can form.

The behavior of gas bubbles in narrow, liquid-filled, gaps has been investigated by organizations interested in sodium-bonded fuel elements.<sup>2-7</sup> The general conclusions were that even without obstructions, stagnant bubbles can form in narrow gaps. When a system of stacked pellets in a cylindrical tube was tested,<sup>4</sup> relatively large bubbles formed under the edges of eccentrically located pellets. Mechanical vibrations were not effective in moving the bubbles located under pellet edges. Although there are many differences between these simulations and real fuel elements (for example, the simulations used liquids other than sodium in most cases, and were isothermal), they provide plausible mechanisms for the formation of gas bubbles in sodium bonds.

The effect of gas bubbles in a sodium bond on the temperature profile near the bubble has also been examined.<sup>5,6</sup> Bubbles which blanket small angles of the fuel surface (less than  $30^\circ$  or about 2 mm width in a fuel element with 8 mm o.d. cladding) do not increase the maximum fuel temperature very much, but the sector of fuel covered by the bubble can run at temperatures much higher than it would if no bubble were present. As the angle blanketed by the bubble increases, the location of the maximum fuel temperature moves from the center toward the fuel surface. For bubble angles greater than about  $60^\circ$ , the maximum fuel temperature is located near the fuel surface, at the center of the bubble. With large bubbles, a significant fraction of the fuel may operate at temperatures above the maximum temperature which would result if no bubbles were present.

In review, there is ample fission gas available to form bubbles in a sodium bond. Also, previous work has indicated a mechanism for trapping bubbles under edges of eccentrically located pellets and has described an observable consequence of large bubbles, i.e. high temperatures

in the fuel under the bubble. In spite of this, there has been no clear evidence for the existence of gas bubbles in the sodium bond of fuel elements examined after irradiation. Levine, et. al.<sup>8</sup> presented a section of a (U,Pu)C fuel element from a thermal irradiation (5 at. % burnup) in which one quadrant of the fuel showed much higher swelling than the other pieces. The high swelling region was bounded by radial cracks in the fuel. They speculated that this region appeared as it did because it was free to swell unrestrained, while the other pieces of the fuel were restrained by the cladding and adjacent fuel fragments. In a later publication,<sup>9</sup> they mentioned the possibility of a gas bubble in the sodium bond outside this region. The boundary of the high swelling region did not follow the outline of isotherms that would result from a bubble in the bond. Thus a clear relation between the high swelling and a bond bubble cannot be made.

During the recent postirradiation examinations of sodium-bonded elements at LASL, a number of asymmetric swelling patterns and asymmetric regions of  $\beta - \gamma$  activity (in autoradiographs) were observed. The swelling patterns were particularly evident in fuel that was originally 98% of theoretical density. Figures 463-1 and 463-2 show photomosaics of two fuel sections. The high-porosity, asymmetric, regions exhibit grain-boundary swelling. The high-density areas visible within the grain-boundary swelling regions are large single grains which show little porosity within the grains. The boundaries of the high-porosity regions are not influenced by the major cracks in the fuel pellets, i.e., the boundaries cross the cracks with little perturbation. If it is assumed that the observed grain-boundary swelling occurs only above some critical temperature, the boundary between the region of high swelling and the region of low swelling should parallel isotherms in the fuel.

Heat transfer calculations were performed to obtain the shape of isotherms in a transverse plane of a fuel element with various size gas bubbles in the sodium bond between the fuel and cladding. The fuel, bond, and cladding were divided into eight radial regions, 24 circumferential regions ( $15^\circ$  each), and three axial layers for numerical heat transfer calculations. Sodium-bond

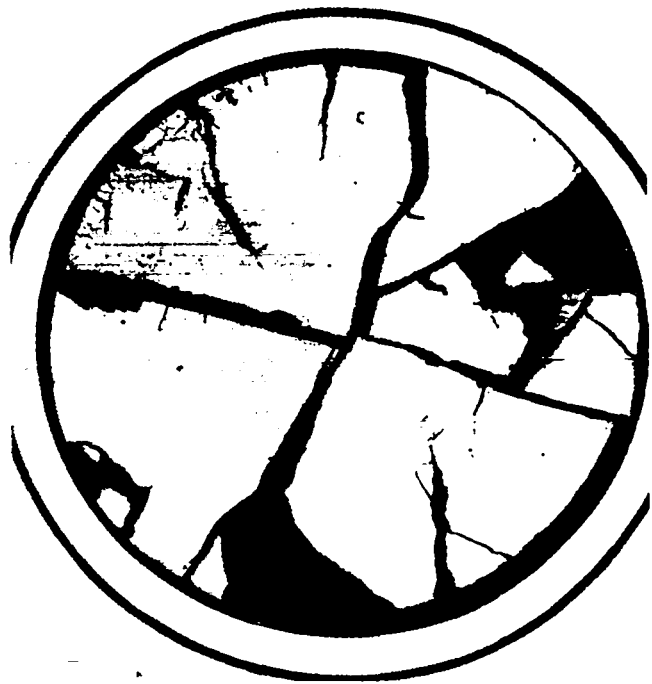


Fig. 463-1. Photomosaic of a high-density, sodium-bonded, carbide fuel element showing asymmetric regions of grain-boundary swelling. (Fuel element U194, Section F; Mount No. 2C8).

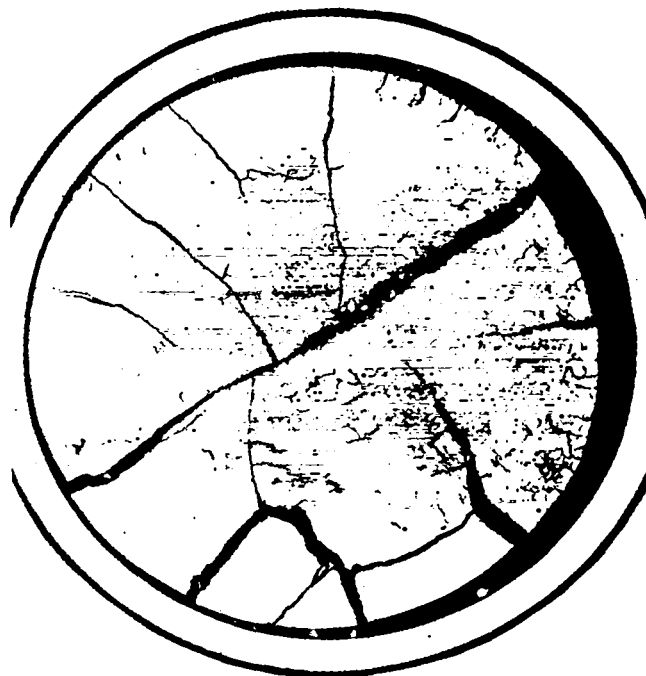


Fig. 463-2. Photomosaic of a high-density, sodium-bonded, carbide fuel element showing swelling resulting from a bubble trapped by an eccentrically-located pellet. (Fuel element U195, Section N; Mount No. 3C92T).

bubbles subtending angles of  $30^\circ$  to  $120^\circ$  were simulated by replacing liquid sodium conductivity with argon gas conductivity in the bubble nodes. Radiation was allowed from the fuel surface to the inside cladding surface through the bubble. Calculations were performed for bubbles with a ratio of circumferential width to axial width of 2, 1, and 0 (infinitely long bubble). Figure 463-3 shows the isotherms at  $80^\circ\text{C}$  intervals in a fuel pellet from an element with a very long,  $60^\circ$ , gas bubble in the sodium bond. A comparison of the isotherm shape with the shape of the high swelling region of Fig. 463-1 shows excellent agreement. Figure 463-4 shows the isotherms at  $80^\circ\text{C}$  intervals in a fuel pellet from an element with a short (axial/circumferential width =  $1/2$ )  $120^\circ$  gas bubble in the sodium bond. The isotherms are from the central plane of the bubble. Their shape compares well with the high porosity region of Fig. 463-2. There is no unique correspondence between the bubble size (circumferential and axial widths) and the isotherm shape. Isotherms similar to those in Fig. 463-3 could also result from an approximately  $75^\circ$  square bubble in the sodium bond. Thus, for any observed high-swelling pattern, a unique bubble size cannot be determined, only a possible size range.

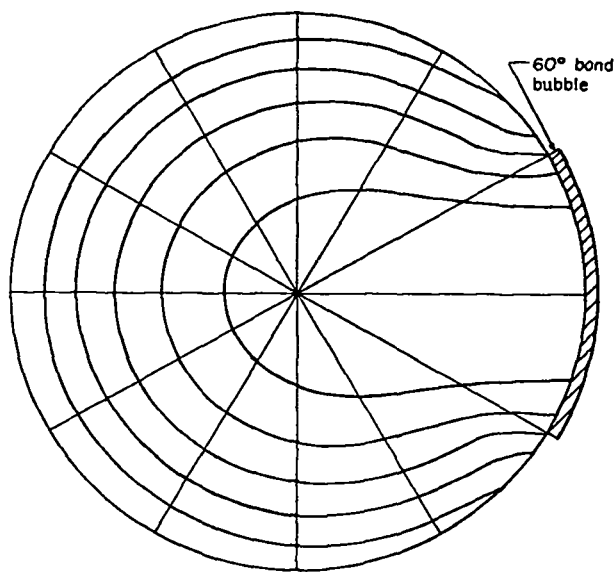


Fig. 463-3. Calculated isotherms at  $80^\circ\text{C}$  intervals in a carbide fuel pellet from an element with a very long,  $60^\circ$ , gas bubble in the sodium bond.

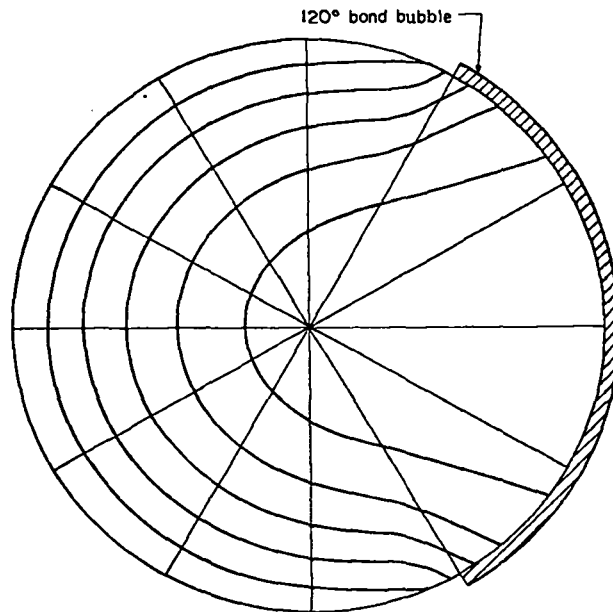


Fig. 463-4. Calculated isotherms at  $80^\circ\text{C}$  intervals in a carbide fuel pellet from an element with a short (axial/circumferential width =  $1/2$ ),  $120^\circ$ , gas bubble in the sodium bond.

The high temperature in the fuel under a gas bubble can also affect fission product migration. Figure 463-5 shows a  $\beta$ - $\gamma$  autoradiograph (the dark areas are high activity) of the section shown in Fig. 463-2. There is a depletion of activity in the center, and in one sector the activity depletion approaches the fuel surface. This sector corresponds to the high porosity region seen in Fig. 463-2. Figure 463-6 shows another  $\beta$ - $\gamma$  autoradiograph with an asymmetric depletion in activity. In this case, the photomosaic of the section did not show a corresponding porosity variation.

The section shown in Fig. 463-2 was examined further to try to obtain some information about the axial variation of the high-porosity region. The section was cut axially on a plane which bisected the region of high porosity. Figure 463-7 shows a photomosaic of the longitudinal section obtained. The bottom corresponds to the plane shown in Fig. 463-2. About  $1/3$  of the pellet with the asymmetric high porosity region is visible on the bottom. The pellet above shows high porosity (grain-boundary swelling) in the center only. This would be expected from a pellet with a continuous sodium bond where the center was the hottest region. The discontinuity in the porosity variation

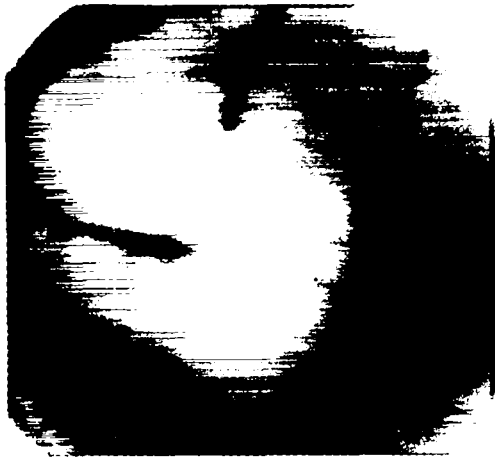


Fig. 463-5.  $\beta$ - $\gamma$  autoradiograph of the fuel element section shown in Fig. 463-2. (Fuel element U195, Section N; Mount No. 3C92T).

across the pellet interface can be explained by assuming that a gas bubble blanketed a portion of the lower pellet but did not extend above the pellet interface. The porosity distribution probably resulted from a bubble trapped under the edge of the upper pellet (See Fig. 7 of Ref. 4).

The photomosaics with asymmetric porosity distributions and the  $\beta$ - $\gamma$  autoradiographs with asymmetric activity regions shown here are presented as evidence that relatively stationary gas bubbles exist in sodium bonds during irradiation. This conclusion is reached since: (1) there is an availability of fission gas; (2) there is a mechanism to hold bubbles in the bond under edges of eccentrically located pellets; and (3) the outline of the asymmetric swelling regions corresponds to the shape of



Fig. 463-6.  $\beta$ - $\gamma$  autoradiograph showing asymmetric depletion of activity. (Fuel element U191, Section M; Mount No. 3C71).

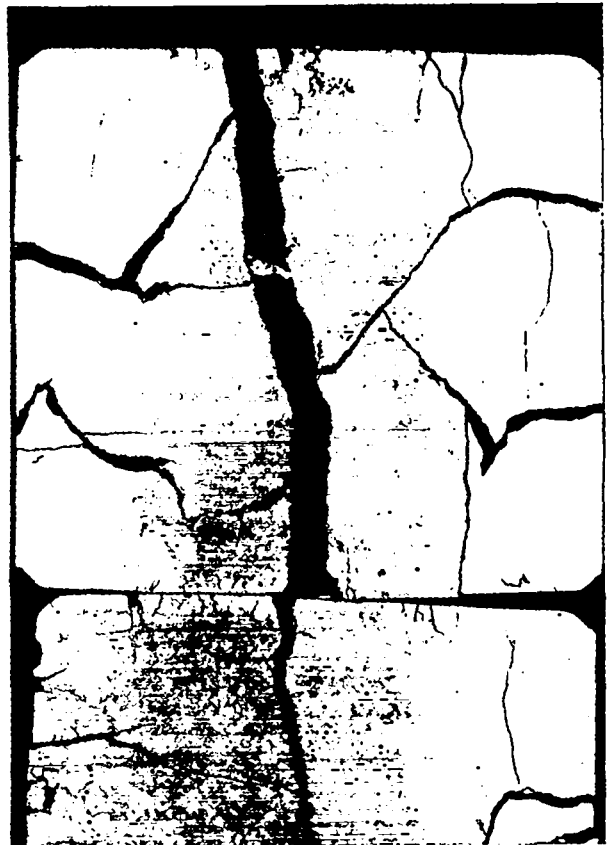


Fig. 463-7. Photomosaic of the longitudinal section associated with the transverse section shown in Fig. 463-2. (Fuel element U195, Section N; Mount No. 3C92L)

isotherms in the fuel if bubbles were present in the bond. The term relatively stationary is difficult to define. The time constant for establishing an asymmetric temperature distribution in the fuel is only a few seconds. The time required for the fuel shown in Figs. 463-2 and 463-7 to swell cannot be determined at this stage of development of advanced fuels.

The pictures shown here represent a sample of more than 10 fuel element sections exhibiting the asymmetric swelling or asymmetric  $\beta$ - $\gamma$  activity phenomenon. As stated earlier, the particular sections shown were chosen because the contrast between the original 98% theoretical density fuel and the high porosity regions is obvious. Other fuels with initial densities below 95% of theoretical also show asymmetric porosity regions resulting from gas bubbles in the sodium bond, but, in many cases, there is little contrast between the regions of high and low

swelling. One observed trend is that the occurrences of asymmetric porosity or activity regions in fuel element sections were greater in elements with larger initial sodium-bond gap widths. Since larger gaps would lead to larger pellet offsets between eccentric pellets, elements having large fuel-cladding gaps may trap gas bubbles in the bond more often than elements with smaller gaps.

The relationship between gas bubbles in the sodium bond of fuel elements and the fuel element failures observed so far is not clear. It is obvious that a gas bubble perturbs the operation of the fuel element, and that large bubbles can cause a significant portion of the fuel to operate above the design temperature. The increased fuel swelling in the region covered by the bubble may decrease the design burnup limit of the element. But evidence of large (covering more than 90° of the fuel surface) gas bubbles has been observed in fuel elements which have not failed at 5 at.% burnup. Also evidence for sodium-bond gas bubbles has been observed in a number of elements classed as slight failures, but the occurrence of gas bubbles has not been related to the failures. Although bond gas bubbles can be considered as harmful to the ultimate potential of sodium-bonded elements, there is no evidence to indicate that they caused any of the initial failures observed to date. The incidence of sodium-bond gas bubbles may be reduced in the future if liner tubes are used. The very small gap between the fuel and the liner tube (less than 0.05 mm) does not permit significant pellet eccentricities. Thus, potential gas bubble traps under edges of eccentric pellets may be eliminated. This postulate should be verified by a comparison of the elements with and without liners in the U5100 Series currently being irradiated.

### III. QUALITY ASSURANCE (L. E. Lanham)

#### General

The major quality assurance effort has been to establish and implement an independent surveillance activity for the Advanced Fuels Program. Surveillance activities are being conducted on a routine basis for all fabrication areas.

#### Fuel Preparation

All corrective actions have been completed on the audit of phototypical fuel element preparation. The quality assurance surveillance activities have resulted in some adjustments in use and documentation of calibrated instruments. The overchecking procedure has been reviewed and discussed in detail with the operators and supervisor. No major change has been required in the documented QA procedures. An Engineering Test Plan for the Development of Fuel and Facilities for Carbide Reactor Experiments has been written and approved.

#### Fuel Pin Fabrication

Some of the procedures for Fuel Pin Fabrication have been written and approved. This includes the procedure for qualification of welds. The end plugs to be used for the qualification of welds have been fabricated and inspected.

Discussions have been conducted with the Shop Department to provide handling procedures and storage facilities for certified materials used in QA fabrications.

Additional QA documentation is being prepared and will be in place before proceeding with Pin Fabrication.

A quality assurance audit was conducted for the Pin Fabrication records, procedures, and facilities. An audit report has been prepared.

### IV. REFERENCES

1. "Quarterly Progress Report on the Advanced Plutonium Fuels Program, July 1-Sept. 30, 1973," Los Alamos Scientific Laboratory report LA-5477-PR, p. 13 (1973).
2. "Quarterly Status Report on the Advanced Plutonium Fuels Program, April 1-June 30, 1968 and Second Annual Report, FY 1968," Los Alamos Scientific Laboratory Report LA-3993-MS, p. 70 (1968).
3. "Quarterly Status Report on the Advanced Plutonium Fuels Program, October 1-December 31, 1967," Los Alamos Scientific Laboratory Report LA-3880-MS, p. 37 (1968).
4. H. O. Schad and A. A. Bishop, "Stationary Gas Bubbles in Narrow Liquid-Filled Gaps," Nuclear Applications and Technology, 8, 261 (1970).

5. E. H. Novendstern and A. A. Bishop, "Temperature Distribution Caused by Gas Bubbles in a Sodium Bonded Fuel Rod," Chemical Engineering Progress Symposium Series No. 92, Vol. 65, p. 131 (1969).
6. R. Schöneberg and H. Ernst, "The Behavior of Gas Bubbles in a Sodium Bonded Carbide Fuel Element in a Fast Reactor," Nuclear Engineering and Design, 21, 65 (1972).
7. L. Rutland, B. H. Cherry, and S. Isreal, "Critical Bubble Size in Sodium-Bonded Ceramic Fuels," Trans. Amer. Nucl. Soc., 10, 471 (1967).
8. P. J. Levine, et. al., "Postirradiation Observations of Sodium-Bonded (U,Pu)C Fuels," Trans. Amer. Nucl. Soc., 13, 606 (1970).
9. B. L. Harbourne, et. al., "The Irradiation Behavior of Sodium-Bonded Mixed-Carbide Fuel Pins," in Proceedings of the Conference on Fast Reactor Fuel Element Technology, R. Farmakes (ed.), American Nuclear Society, p. 869 (1971).

## PROJECT 472

### FBR ANALYTICAL QUALITY ASSURANCE STANDARDS AND METHODS

#### RESEARCH AND DEVELOPMENT

Person in Charge: R. D. Baker  
Principal Investigator: G. R. Waterbury

---

#### I. INTRODUCTION

Necessary to the development of high quality fuels, control rods, and other reactor components required by the FBR program are highly reliable analytical methods for the chemical characterization of the source materials and products, and for the measurement of burnup, O/M ratio, and various gases on irradiated fuels. Tasks for ensuring the production of these materials are: (1) the continual preparation and distribution of carefully characterized calibration materials and quality control samples for use by the vendors and purchasers and for the surveillance of vendors and purchasers during periods of production, (2) the preparation and guidance in the use of quality assurance programs for chemical specification sampling and analysis, (3) the development of improved methods of analysis, as required, (4) the preparation of continually updated compilations of analytical methods, and (5) the analysis, in a referee capacity, of samples in dispute between vendors and purchasers. For the near future, these tasks are dedicated to the FFTF. They will be extended, as appropriate, to the LMFBR demonstration and large production facilities.

Tasks concerned with irradiated FBR fuel examinations are: (1) the development of burnup methods based on conventional mass spectrometry, on chemical analysis using inexpensive chemical apparatus, and on spark source mass spectrometry for rapid, precise measurements, (2) the prooftesting of developed methods for burnup jointly with the Allied Chemical Corporation (Idaho), (3) the

development of methods for the measurement of the O/M ratio, and (4) the development of methods for the measurement of gases including techniques to measure the release rates of various gases as a function of temperature-time cycling.

As a high priority item, a program has been initiated to establish a quality assurance program and to develop analytical methods, as necessary, for the chemical characterization of low-friction, hard surfaces to be applied to various FFTF core components. Also initiated is a task to prepare a manual of analytical methods for the chemical characterization of metallic core components for issuance as an RDT Standard.

#### II. ANALYTICAL CHEMISTRY PROGRAM FOR LOW-FRICTION, HARD SURFACES

In August of this year, LASL began a cooperative effort with HEDL to establish a program for the chemical characterization of low-friction hard surfaces to be applied to contacting components of the FFTF reactor. The hard surface is to be chromium carbide applied as a molten blend of  $\text{Cr}_3\text{C}_2$  and nichrome powders.

##### A. Development of Analytical Methods

(W. H. Ashley, D. W. Steinhaus, J. E. Rein,  
G. R. Waterbury)

Methods used by a potential vendor for the chemical characterization of  $\text{Cr}_3\text{C}_2$  powder, nichrome powder, and the hard surface were evaluated, and, in general, proved to be basically sound. Several methods were modified for improved analysis rates and precisions, and methods

for several components, not previously determined, were developed. Final prooftesting of all methods used actual samples including a typical hard surface test specimen.

1. Dissolution of Samples  
(R. D. Gardner, R. E. Perrin)

The potential vendor has used  $\text{Na}_2\text{O}_2$  fusion for the dissolution of  $\text{Cr}_3\text{C}_2$  and hard surface preceding chemical analyses for the major and minor components. This operation is labor consuming and requires the attention of a skilled analyst. As reported previously,<sup>1</sup> complete dissolution of  $\text{Cr}_3\text{C}_2$  (and of nichrome) was effected using  $\text{HClO}_4$  or  $\text{HClO}_4$  plus a small quantity of  $\text{HNO}_3$  under reflux conditions in a fused-silica apparatus. Further studies showed that the recovery of chromium was slightly low when  $\text{HNO}_3$  was present. The test specimen of hard surface dissolved completely with  $\text{HClO}_4$  alone. Dissolution with only  $\text{HClO}_4$  is recommended as the "universal" system for  $\text{Cr}_3\text{C}_2$ , nichrome, and hard surface samples to be analyzed for the various specification components. One exception, discussed in section 3, is the dissolution of samples for nitrogen determination.

2. Determination of Chromium  
(R. E. Perrin, R. D. Gardner)

The basis of this determination is the formation of  $\text{Cr}^{6+}$ , the addition of a known quantity of  $\text{Fe}^{2+}$  in excess, and the titration of the unreacted  $\text{Fe}^{2+}$  with standard  $\text{Ce}^{4+}$  solution to a potentiometric end point. Dissolution of the sample with  $\text{HClO}_4$  under reflux incompletely oxidizes the Cr to  $\text{Cr}^{6+}$ . Manganese, an impurity in the materials analyzed, causes a positive bias. For these reasons, a modified method was developed.

The following are the major sequential operations of the modified method: (1) following the dissolution of the sample with  $\text{HClO}_4$ , the solution is diluted and boiled to expel most of the free chlorine, (2)  $\text{Ag}^+$  and  $(\text{NH}_4)_2\text{S}_2\text{O}_8$  are added, and the solution is made 0.3 to 0.5M in  $\text{HNO}_3$  and then is heated to remove any remaining free chlorine by precipitation of  $\text{AgCl}$  and to complete the oxidation of Cr to  $\text{Cr}^{6+}$ , (3)  $\text{HCl}$  is added and the solution is boiled to reduce any  $\text{Mn}^{7+}$  to noninterfering  $\text{Mn}^{2+}$ , and (4) excess  $\text{Fe}^{2+}$  is added and titration is made with  $\text{Ce}^{4+}$ .

3. Determination of Nitride Nitrogen  
(R. E. Perrin)

A method developed for this analysis includes acidic dissolution of the sample, addition of  $\text{NaOH}$ , distillation of the  $\text{NH}_3$  that is produced into a boric acid solution, and titration with standard acid. Recovery of  $\text{NH}_3$  is low and erratic when samples are dissolved in  $\text{HClO}_4$ . It is possible that nitride nitrogen is partially oxidized either to nitrate or to some volatile nitrogen species that escape from the reflux condenser. Quantitative recovery is being attempted by using 12M  $\text{H}_2\text{SO}_4$  as the solvent with the sealed fused-silica tube apparatus at  $500^\circ\text{C}$  for 24-h reaction periods.

4. Determination of Metal Impurities  
(O. R. Simi)

An emission spectrographic method has been developed for the determination of general metal impurities in the hard surfaces. A sample is dissolved in  $\text{H}_2\text{SO}_4$  plus a small amount of  $\text{HNO}_3$  in a Teflon beaker. The resulting solution is evaporated to dryness and ignited in air to an oxide matrix. A weighed aliquot is placed in a cratered graphite electrode and excited by a dc arc in a 60% Ar-40%  $\text{O}_2$  atmosphere. Reference standards consist of a series of powder blends of chromium and nickel oxides with graded concentration levels of the various impurity metal oxides. The Ni/Cr ratio of the reference standard series matches that of the hard surface sample.

B. Chemical and Electron Microprobe Characterization of Hard Surface  
(E. A. Hakkila, W. H. Ashley, D. W. Steinhaus)

To provide information as a guide for chemical specifications for a HEDL document of specifications for the hard surface, a test sample of hard surface provided by the potential vendor was extensively analyzed at LASL. This test sample consisted of a brass tube coated with hard surface. The sample that is planned for chemical specification overcheck analyses during production periods will differ by the use of an aluminum tube as the base for the applied hard surface. In the extensive analysis of the hard surface test specimen, Cu and Zn, the major components of brass, were determined. This was necessary because the hard surface, physically separated from the brass cylinder, had adhering brass fragments

and one objective of the analysis was a total material balance.

Table 472-I lists the analytical results for 11 elements determined chemically. As discussed above, Cu and Zn are brass components. Noteworthy is the significant oxygen content of slightly more than 1 wt%.

Thirty elements were determined by the emission spectrographic method described in the previous section on two samples, one with adherent brass and the other after the adherent brass was removed with HNO<sub>3</sub> leaching. On the brass-free sample, no metallic elements other than those listed in Table 472-I were present in substantial quantities. Elements present above detection limits, in units of micrograms per gram of hard surface, were Mg-7, Al-125, Ca-50, Ti-25, V-25, Cu-125, and Ba-140.

The major results of the electron microprobe analysis were: (1) brass (Cu and Zn) had not diffused into the hard surface, (2) Cr and Ni diffused to a depth of about 10 μm into the brass cylinder, (3) the hard surface had two phases, (4) the major phase was a heterogeneous mixture of Cr, Ni, and C, (5) the minor phase, generally < 5 μm wide, was Ni and Cr void of C.

TABLE 472-I  
CHEMICAL ANALYSIS OF HARD SURFACE  
TEST SPECIMEN

Element	Wt% <sup>a</sup>	Std Dev <sup>b</sup>
Cr	73.42	0.08
Ni	15.77	0.04
Fe	0.33	0.10
Mn	0.11	0.006
Co	< 0.05	--
Cu	0.51	0.05
Zn	0.24	0.04
Si	0.095 (1)	--
N	0.44 (2)	--
C	7.08	0.06
O	1.10 (2)	--

(a) <sup>a</sup> Average of results for three separately dissolved samples, unless indicated otherwise with the number of determinations in parenthesis after the result.

<sup>b</sup> Expressed as the value for a single determination calculated from the three results.

C. Round Robin Evaluations of Analytical Capabilities  
(J. E. Rein, R. K. Zeigler, G. R. Waterbury)

The procurement by HEDL of lots of nichrome powder, Cr<sub>3</sub>C<sub>2</sub> powder, and hard surface, the materials that are to serve as the round robin samples, is delayed until January. Packaging and distribution of the samples to the participating laboratories will require a minimum of two weeks after receipt of the materials at LASL.

D. Analytical Method Manual

The joint preparation was started by HEDL and LASL of a manual of analytical methods for chemical specification analysis of hard surface. To expedite the task, each laboratory will prepare initial drafts of approximately half of the designated methods which will be exchanged. The goal for completing the first drafts is mid-January.

E. Reference and Quality Control Materials  
(J. E. Rein, G. R. Waterbury)

In the FFTF Quality Assurance plan for the hard surface program, the initial reference materials for the chemical methods of analysis will be NBS Standard Reference Materials supplemented by designated high-purity materials. These materials have been selected and HEDL has been supplied with information necessary for their procurement.

The planned reference materials for later in the program will be lots of Cr<sub>3</sub>C<sub>2</sub> powder, nichrome powder, and hard surface used for the round-robin method evaluation provided they prove homogeneous. The use of quality control samples is to be implemented later in the program. The planned materials for this purpose are lots of hard surface with varying proportions of the Cr<sub>3</sub>C<sub>2</sub> and nichrome powders. HEDL estimates procurement of these lots by the end of this fiscal year. Characterization of these lots is estimated to require three months.

III. ANALYTICAL CHEMISTRY PROGRAM FOR METALLIC CORE COMPONENTS  
(W. H. Ashley, E. A. Hakkila, M. E. Smith, J. E. Rein, G. R. Waterbury)

As a new task, LASL has joined HEDL in the preparation of RDT Standard F11-3 "Analytical Chemistry Methods for Metallic Core Components." This document will present a series of detailed methods for the

determination of major and minor elements in various alloys of stainless steel and Inconel. Potentially applicable methods are being reviewed by personnel of the two laboratories.

#### IV. ANALYTICAL CHEMISTRY PROGRAM FOR BORON CARBIDE

##### A. Status of Analytical Methods and Qualification of Analytical Laboratories

(J. E. Rein, R. K. Zeigler, W. H. Ashley,  
G. R. Waterbury)

As stated last quarter,<sup>1</sup> all methods presently recommended in RDT F11-2 for FFTF chemical specification analyses are deemed satisfactory. The development of a more reliable dissolution procedure for boron carbide preceding the total boron determination is presented in Section C.

##### B. Calibration and Quality Control Materials

(J. V. Pena, H. J. Kavanaugh, L. A. Maestas,  
J. E. Rein)

Last quarter, boron carbide pellets designated as calibration material for the total-boron analytical method were packaged and sent to HEDL. All calibration and quality control materials deemed adequate for the initial production of FFTF boron carbide pellets have now been sent to HEDL.

##### C. Development of an Improved Dissolution Procedure for the Determination of Total Boron

(R. E. Perrin, W. H. Ashley)

The present dissolution procedure for  $B_4C$  given in RDT F11-2, involving a  $Na_2CO_3$  fusion, is prone to low recovery, and requires close attention of a skilled analyst. The dissolution procedure based on reaction with  $12M$   $H_2SO_4$  in sealed fused-silica tubes was further evaluated. As previously reported,<sup>1</sup> a reaction temperature of  $500^\circ C$  was selected based on the observation that one lot of  $B_4C$  did not completely dissolve at lower temperatures. This set of conditions gave quantitative recovery of total boron in Carborundum Lot 3 Naval Standard  $B_4C$  and gave total boron results for a lot of  $B_4C$  pellets that agreed with the results obtained after dissolution by the  $Na_2CO_3$  fusion procedure.

A major objective of the further evaluation was to intercompare total boron assay results for the two dissolution treatments on a wider variety of boron carbide

materials. Unexpectedly, the results for the  $B_4C$  that resisted dissolution with  $12M$   $H_2SO_4$  at temperatures less than  $500^\circ C$  were 0.5% low compared to the results obtained on  $Na_2CO_3$  fused samples. The recovery decreased even further with increased reaction temperatures. This effect may be unique for this particular lot of boron carbide, known to contain 0.7 wt% zirconium.

#### V. ANALYTICAL CHEMISTRY PROGRAM FOR FBR MIXED OXIDE FUEL

##### A. Calibration Materials and Quality Control Samples

(J. V. Pena, H. J. Kavanaugh, L. A. Maestas,  
J. E. Rein)

The packaging of calibration materials and quality control samples that presently are available for shipments C and D (nominal shipment dates of December 1973 and March 1974) is nearing completion. However, the available supply of certain mixed oxide and plutonium oxide calibration and quality control blends is not adequate to complete the packaging. HEDL has informed us that suitable matrix materials required for the preparation of these blends will be shipped starting early in January. Characterization, blend preparation, and packaging require about three months; hence, a shortage of these blends appears likely.

##### B. Development of Analytical Methods

###### 1. Determination of Burnup

- a. Study of Chemical Separation Procedure for Burnup Determination by Mass Spectrometry  
(S. F. Marsh, M. R. Ortiz,  
R. M. Abernathy, J. E. Rein)

The two-column, ion-exchange procedure<sup>2</sup> was modified to improve reliability and decrease analyst effort. In this procedure, the first column retains Pu and U as anionic chloride complexes from  $12M$  HCl while Nd and most other fission products pass through. The second column chromatographically separates Nd from other fission products, including rare earths, as anionic nitrate complexes using a methanol- $HNO_3$  mixed solvent. The Pu and U are sequentially eluted from the first column with  $0.1M$ -HI- $12M$  HCl followed with  $0.1M$  HCl.

The major modifications are: (1) substitution of macroporous anion exchange resin for the previously used conventional ion exchange resins in both columns, (2) a

change in the composition of the methanol-HNO<sub>3</sub> mixed solvent for the neodymium chromatographic separation, and (3) automation of the chromatographic column operation. A LASL report is in preparation describing technical aspects of the modifications and presenting a detailed description of the procedure as it currently is used.

b. Development of Burnup Method Using Conventional Low-Cost Apparatus  
(S. F. Marsh, M. R. Ortiz, J. E. Rein)

This measurement of burnup incorporates an ion exchange separation of U, Pu, and total rare earths (as the fission product monitor) with a spectrophotometric measurement of each. The separation procedure, based in part on the two-column, ion-exchange procedure described above, involves fuming the sample with HClO<sub>4</sub> to oxidize Pu to Pu<sup>6+</sup> prior to retention of U and Pu on a macroporous anion exchange column from 12M HCl. The effluent which contains trivalent actinides, rare earths, and most other fission products, is converted to an ethanol-HCl medium and transferred to a pellicular cation exchange resin column. The rare earths are sorbed while trivalent actinides (Am and Cm) and extraneous fission products pass through.<sup>3</sup> The rare earths then are eluted with 5M HCl. Plutonium and uranium are sequentially eluted from the first (anion exchange) column with 0.1M HI-12M HCl, followed by 0.1M HCl.

Arsenazo III has been selected as the chromogenic agent for the spectrophotometric measurement of the isolated uranium, plutonium, and total rare earths. Problems of erratic color intensity with standards and high blank absorbance encountered initially appear to have been overcome by extensive repurification of the Arsenazo III coupled with a reduction in the amount of this reagent added.

The rare earth-Arsenazo III complex, developed at pH 2.9 using chloroacetate buffering, exhibits maximum absorbance at 660 nm. The molar absorptivity for the complex of 50,000 is sufficiently large to permit the use of small-size irradiated samples such that shielded facilities will not be required.

Uranium forms a stronger Arsenazo III complex than is formed with the rare earths. This allows the

colored complex to be developed at a low pH at which few metal ions react with Arsenazo III. The uranyl-Arsenazo III complex, developed at pH 1.7 using maleate buffering, has an absorbance maximum at 652 nm and a molar absorptivity of almost 60,000. The selectivity is increased by incorporating ethylenediaminetetraacetic acid (EDTA) masking. An EDTA concentration of 0.01 wt%, relative to the final 25 ml of solution, depresses the uranium complex absorbance by only 5% and effectively masks Zr. Zirconium is a major fission product element that will accompany U in the extraction and that forms an extremely strong Arsenazo III complex.

c. Determination of O/M Ratio in Solid Solution (U,Pu)O<sub>2</sub>  
(G. C. Swanson, G. R. Waterbury)

The apparatus used to calibrate thermogravimetric methods for the determination of the O/M ratio in (U,Pu)O<sub>2</sub> fuels consists of a ceramic electrochemical cell for the production of gases with varying oxygen potentials and a Mettler recording thermobalance installed in a glovebox. Recently, the ceramic cell failed due to thermal shock. Because these types of cells are fragile, alternate and more robust systems for oxygen gas generation are being evaluated.

The thermobalance, high-vacuum system has been overhauled extensively prior to its use on plutonium materials. It is now ready for the preparation of a U-Pu solid solution oxide of known oxygen content. Highly pure uranium and plutonium metals will be melted together in the thermobalance to prepare a U-Pu alloy followed by a controlled oxidation.

D. Development of Gas Measurement Techniques  
(R. M. Abernathy, J. E. Rein)

Assembly has been completed of an apparatus that is designed to measure gas components as they are released from samples of fuel, B<sub>4</sub>C, and other LMFBR/FFTF materials as a function of temperature. Testing of the apparatus is delayed pending the installation of electrical power required for operation of the apparatus.

VI. QUALITY ASSURANCE  
(L. E. Lanham)

A quality assurance audit was conducted of the procedures and records for the preparation of calibrated

materials and quality control analytical samples. The audit determined this operation meets all of the requirements of the CMB-RRD Quality Assurance System. An audit report has been prepared.

This project is included in the surveillance activities of the quality assurance organization.

#### VII. REFERENCES

1. R. D. Baker, "Quarterly Report -- Advanced Plutonium Fuels Program July 1 to September 30, 1973," Los Alamos Scientific Laboratory report LA-5477-PR (December 1973).
2. R. M. Abernathy, G. M. Matlack, and J. E. Rein, "Sequential Ion Exchange Separation and Mass Spectrometric Determination of  $^{148}\text{Nd}$ , Uranium, and Plutonium for Burnup and Isotopic Distribution Measurements," in Analytical Methods in the Nuclear Fuel Cycle, Vienna, 1972 (International Atomic Energy Agency), Paper IAEA-SM149/37, STI/Pub/291, pp. 513-521.

3. S. F. Marsh, M. R. Ortiz, and J. E. Rein, "Lanthanide-Trivalent Actinide Separations in Ethanol-Hydrochloric Acid," presented at the 17th Conference on Analytical Chemistry in Nuclear Technology, Gatlinburg, TN, October 23-25, 1973.

#### VIII. PUBLICATIONS, TALKS

1. R. K. Zeigler, "Quality Assurance Plan for Mixed Oxide Fuel for LMFBR," presented at the 20th Western Regional Conference, American Society for Quality Control, Portland, OR, September 27-29, 1973.
2. O. R. Simi (LASL) and R. Ko (HEDL), "The Spectrographic Determination of Metal Impurities in Boron Carbide," presented at the 1973 Pacific Conference on Chemistry and Spectroscopy, San Diego, CA, November 1-3, 1973.
3. S. F. Marsh, M. R. Ortiz, and J. E. Rein, "Lanthanide-Trivalent Actinide Separation in Ethanol-Hydrochloric Acid," presented at the 17th Conference on Analytical Chemistry in Nuclear Technology, Gatlinburg, TN, October 23-25, 1973.